84 pages

IN-27

JPL PUBLICATION 85-101

IN-14288

The Effects of Energetic Proton Bombardment on Polymeric Materials: Experimental Studies and Degradation Models

Daniel R. Coulter
Amitava Gupta
Mark V. Smith
Jet Propulsion Laboratory

R.E. Fornes
North Carolina State University

JJS 7/4/50

N3841777

June 1, 1986

NASA
National Aeronautics and Space Administration

Jet Propulsion Laboratory
California Institute of Technology
Pasadena, California

JPL PUBLICATION 85-101

The Effects of Energetic Proton Bombardment on Polymeric Materials: Experimental Studies and Degradation Models

Daniel R. Coulter
Amitava Gupta
Mark V. Smith
Jet Propulsion Laboratory

R.E. Fornes
North Carolina State University

June 1, 1986

NASA
National Aeronautics and
Space Administration

Jet Propulsion Laboratory
California Institute of Technology
Pasadena, California

The research described in this publication was carried out by the Jet Propulsion Laboratory, California Institute of Technology, under a contract with the National Aeronautics and Space Administration.

ABSTRACT

This report describes 3 MeV proton bombardment experiments on several polymeric materials of interest to NASA carried out on the Tandem Van De Graff Accelerator at the California Institute of Technology's Kellogg Radiation Laboratory. Model aromatic and aliphatic polymers such as poly(1-vinyl naphthalene) and poly(methyl methacrylate), as well as polymers for near term space applications such as Kapton, Epoxy and Polysulfone, have been included in this study. Chemical and physical characterization of the damage products have been carried out in order to develop a model of the interaction of these polymers with the incident proton beam. The proton bombardment methodology developed at the Jet Propulsion Laboratory and reported here is part of an ongoing study on the effects of space radiation on polymeric materials. The report is intended to provide an overview of the mechanistic, as well as the technical and experimental, issues involved in such work rather than to serve as an exhaustive description of all of the results.

TABLE OF CONTENTS

TABLE OF CONTENTS (Continued)

LIST OF TABLES

LIST OF FIGURES

LIST OF FIGURES (Continued)

LIST OF FIGURES (Continued)

I INTRODUCTION

The advent of the Space Shuttle has brought about radical changes in design concepts for current and future spacecraft. One of the major new thrusts is the movement away from totally metallic structures and toward the utilization of organic polymers in such applications as optical coatings, thermal control components, and composite matrix materials. A major issue that must be addressed in order to effectively implement these new design concepts is a determination of the effects of space radiation over an extended period of time on the properties of these polymeric materials.

Prior to operation of the Space Shuttle, spacecraft were engineered to withstand the severe stresses encountered during launch. In light of the short term (< 5 years) nature of most missions, this resulted in an inherently large design margin for the relatively small stresses encountered in space operation. Availability of the Space Shuttle has made it possible to put into orbit very large space structures (i.e., Space Station) which, because they are not transported totally intact, but rather are fabricated, assembled, or unfolded in space, encounter significantly reduced launch loads. In order to be technically and scientifically attractive as well as cost effective, future space structures will have to be designed to withstand space operational loads (rather than launch loads) and to operate for long lifetimes (10-30 years).

A major uncertainty inhibiting the development of efficient long term designs is the effects on the optical, chemical, physical, and mechanical properties of various polymeric materials due to prolonged exposure to space radiation. The body of currently available information in this area, though growing, is still insufficient to assess reliably the performance of a material in a given environment over an extended period of time. In order to develop the necessary design and material selection criteria, major test facilities are

required. The practicalities of facility construction, test execution, and timely generation of data require significant deviation from the actual space radiation environment (accelerated testing). In order to design these engineering tests to yield reliable data in the time available and at a reasonable cost, they must be accompanied by research efforts to understand the nature and rates of the basic mechanisms that underly the deleterious effects of space radiation on polymeric materials.

The radiation environment encountered in earth orbit consists primarily of solar electromagnetic radiation (γ-ray, X-ray, UV, visible, IR) and solar wind particles (electrons, protons, α-particles, etc.) which have been trapped in the magnetic field of the earth. The exact nature of the environment depends strongly on the orbital altitude, the inclination of the orbital plane to the equatorial plane of the earth, and on the level of solar activity. A significant component of the radiation environment encountered by spacecraft orbiting at most all altitudes above 250 km are energetic (.1-10 MeV) protons. For example, polymeric surfaces on a vehicle orbiting at 800-1000 km could be exposed to hundreds of Mrads of such proton radiation over a 30 year lifetime. At higher orbits, the accumulated dose could increase by as much as three orders of magnitude. Clearly, testing programs to evaluate materials exposed to such environments are necessary if the proposed lifetime goals of long term missions are to be met.

This report describes an initial effort to investigate some of the basic interactions of energetic protons on polymeric materials. The radiation exposure was carried out at the Kellogg Radiation Laboratory of the California Institute of Technology. The effects of energetic protons on five polymeric materials including Kapton, polysulfone (Udell 1700), epoxy (NARMCO 5208), PMMA, and poly(1-vinylnaphthalene) (P1VN) have been investigated. The report

is divided into six sections: Introduction, Technical Background, Approach, Experimental, Results, and Conclusions. The first section states the scope of the problem and describes the rationale for investigation. The second section gives a brief review of the state of knowledge concerning the effects of radiation (specifically proton radiation) on polymers. The third section describes the framework within which results will be interpreted and delineates key considerations in the development of test methodology. The fourth section describes test design and experimental details. The fifth section presents observations, results, and analysis of the data gathered in the experiments and finally, the last section lists some general conclusions on the effects of protons on organic polymeric materials as well as some important considerations relevant to design of engineering tests.

II TECHNICAL BACKGROUND

Ionizing radiation in the form of high energy photons (X-rays, γ-rays) or energetic particles (electrons, protons, neutrons, α-particles, etc.) incident on organic polymers can produce significant changes in the chemical, physical, and mechanical properties of these materials. As early as 1952, Charlesby found that mild "pile irradiation" of solid polyethylene produced an infusible, insoluble, rubberlike material.[1] Further, larger doses of radiation reduced the polymer to a brittle, discolored, glassy substance.[2,3,4] Studies on a number of other polymeric materials including nylon,[4] polystyrene,[4,5] poly(vinyl chloride),[5] poly(vinyl bromide),[5] etc., showed similar results. It was found, however, that some polymers behaved quite differently when irradiated. A combination of γ-ray and neutron bombardment of poly(methyl-methacrylate), for example, reduced the material to a crumbly white powder.[6] Poly(tetra-fluoroethylene)[2] and poly(iso-butylene)[2,7] also underwent extensive degradation.

Early testing on a large number of substances led to the conclusion that organic polymers show two general types of behavior upon radiolysis. In those like polyethylene, radiation promotes the formation of new carbon-carbon bonds between adjacent molecules or between different portions of the same macro-molecule (crosslinking). Other materials such as PMMA, Teflon, etc., do not crosslink, but rather undergo bond cleavage or depolymerization which results in the lowering of the average molecular weight of the material. To what extent these processes occur depends largely on the nature of the material and on its physical state (temperature, phase, etc.).

Radiation affects materials by deposition of energy in a series of discrete interactions, each energetic enough to generate a variety of short-lived, reactive species (ions, free electrons, radicals, excited electronic

states, etc.). The quantity and type of intermediates formed, as well as the kinetics of their formation and decay, control the chemical and physical changes that occur in the material. Incident particles interact primarily with atomic electrons in the material. The density of ionization and electronic excitation is typically several orders of magnitude higher for heavier particles than for electrons, due primarily to the fact that their ranges are less.

The initial event in γ-ray or electron radiolysis is usually ionization. High concentrations of electrons, anions, and cations are generated very rapidly ($< 10^{-12}$ s).[8] At room temperature, some of these primary species are difficult to observe directly due to their short lifetimes. At low temperatures, however, some of them are stable. Trapped electrons have been identified in polymer matrices from their ESR[9] and optical absorption[10] spectra following low temperature γ-irradiation. These techniques have also been used in a few cases to study trapped anions and cations in polymers. Geuskens et al[11] studied the production, trapping, and recombination of radical ions by ESR spectroscopy in γ-irradiated PMMA doped with ethyl mercaptan at 77 K. The optical absorption spectra of biphenyl cations, anions, and trapped electrons have also been obtained following low temperature irradiation of biphenyl doped polyethylene.[12]

Many of the ions produced during radiolysis are in an excited state and are unstable. Some of them dissociate rapidly ($< 10^{-9}$ s) into free radicals or molecular fragments (bond breaking processes). These species, which tend to be longer lived than the ions and which may migrate extensively through the polymer,[13] are responsible for a large part of the chemistry that occurs. Free radicals have been observed and identified in a number of irradiated polymers. It is known from ESR,[14] ultraviolet,[15] and infrared[16] absorption measurements

on irradiated polyethylene that alkyl, allyl, and dienyl radicals are formed. Within each class, as many as five distinct species have been identified. Radicals have also been detected in PMMA,[17] polystyrene,[18] poly(vinyl chloride),[19] and many other materials. The radicals that are formed during radiolysis will ultimately recombine (some after very long times, i.e., hours or days) to form new chemical bonds in the polymer or stable chemical products.

The ions that do not dissociate immediately eventually combine with other ions or electrons and, in some cases, generate excited electronic states from which chemistry can also occur. Luminescence is seen during irradiation of most organic polymers. Phillips and Schug,[20] for example, observed fluorescence, phosphorescence, and excimer emission from a number of polymers with aromatic side groups during irradiation with 1 MeV electrons. Investigators in early scintillation research found that excited states produced by irradiation of polymeric materials such as polystyrene[21] and polyvinylnaphthalenes[22] transfer energy efficiently to fluorescent solutes. More recent work has shown that excited states produced in polymers with aromatic side groups can also migrate along the polymer chain until they are trapped, annihilated, or otherwise deactivated.[23,24,25,26]

Radiolysis experiments on polymers with protons or heavier nuclei are less well documented than those with electrons or γ-rays. It is known that both the mechanisms and results of proton irradiations are somewhat different than with electrons. Protons, being much more massive, produce a much higher density of ionization and excitation of atomic electrons, as well as causing enormously more displacement of entire atoms within the bulk material. A few studies have yielded a variety of results. For example, the formation of unsaturation in polyethylene with proton[27] and α-particle[28] irradiation is much faster than with γ-irradiation. Comparative studies on degradation of PMMA

suggest that ^{60}Co γ-rays are twice as damaging as 14 MeV deuterons and more than an order of magnitude more destructive than 28 MeV α-particles[29] in bulk samples, presumably because of the far longer range of the γ rays. Physical property studies on proton irradiated polysulfone have shown that irradiation results in crosslinking and chain scission which lead to changes in material properties such as modulus and Tg.[30] Since relatively little is known about the details of proton irradiation damage to polymers, this study of several representative materials was initiated with two goals in mind: first, to determine what gross chemical and physical changes occur in the polymers due to proton bombardment, and second, to determine the nature of the intermediates produced during radiolysis and measure the rates of formation and decay of these intermediates. With this information in hand, models of degradation due to proton irradiation can be developed for specific materials.

III APPROACH

In some respects, the effects of various types of ionizing radiation on polymers are the same. In all cases, secondary electrons, resulting from the ionization of atoms in the material, play an important and presumably similar role in the radiation chemistry. Thus it is expected that some of the reactive intermediates and some of the chemical changes found to result from proton radiolysis will be the same as those in electron irradiation experiments. It is known, however, that the contribution of secondary electrons to the deceleration of energetic particles decreases in the order: electrons > protons > α-particles.[31] For slow, heavy particles, scattering of atomic nuclei plays an important role in the deceleration process. In addition, as has been mentioned earlier, the formation of damage tracks in insulators is usual for heavy particles,[32] and essentially unknown for electrons. These differences in interaction mechanism may be responsible for the differences observed in radiolysis with heavier particles.

Accelerated electrons incident on a material promote primarily "vertical" transitions. That is, the electron distribution about the atom or molecule changes without significant motion on the part of the nuclei. These primary, excited ionic or electronic states decay into a relatively small set of secondary intermediates. Time resolved spectroscopic studies on PlVN films at JPL, following pulse radiolysis with 600 keV electrons, have led to the observation of only four excited electronic states.[33] Two of these are the napthalene-like, lowest singlet and triplet excited states of PlVN and the other two are intramolecular singlet excimer states. EPR experiments have identified a single persistent radical intermediate produced by electron bombardment of PlVN.

Frequently, the kinds of chemical changes that occur in polymers as a result of electron irradiation are limited. For example, in some cases only certain types of crosslinks are formed; in other cases only depolymerization leading to monomer formation occurs, or bond-specific side-chain cleavage, giving rise to a limited number of volatile products results. Such behavior is non-statistical in the sense that only certain kinds of bonds are broken or formed, only certain intermediates are produced, and only certain reaction pathways are followed. It is the specific nature of the electron interactions with the material, rather than the density of certain chemical "sites" or the energetics of the various processes, that usually determines what chemistry will occur. It is not always the most numerous or weakest bonds that are affected. By comparing C-C and C-H bond energies one would expect that main chain scission in polymers would be more probable than splitting off of hydrogen atoms. In many instances, however, cleavage of C-H bonds is greatly predominant during electron bombardment.

The situation is likely quite different under irradiation with heavier particles. The much higher ionization and electron excitation densities, and the displacement of atoms within the material are expected to produce effects that could greatly alter the chemistry. For example, the large increase in the local density of ionization and excitation will enhance the effects of bimolecular processes by increasing the likelihood and rate of recombination of ions. Furthermore, collisions of the heavy bombarding particles with atomic nuclei in the material may result in non-vertical transitions and significant local heating because of translation-vibration and translation-rotation energy transfer processes.

The number and variety of molecular fragments and radicals can be expected to increase under proton irradiation. As discussed previously, local heating will result in the thermal activation of new bond breaking processes and reactions. In some cases, however, the effects of non-vertical transitions (transitions involving the translation of nuclei) may be important. Very slight motions ($\gtrsim$ 0.1 nm) of the atoms in the polymer matrix, caused by damage track formation by the heavy accelerated particles, will break most chemical bonds. Presumably, these displacement-induced bond-cleavage processes, if they occur, will result in a "statistical" distribution of fragments (H atoms, CH, CH_2, larger species). The distribution will probably be a function of the mass of the fragments, the energy of the bonds broken, and the number of chemical sites from which each fragment can be generated.

Subsequent reactions of these many different species generated during radiolysis will give rise to a wide variety of chemistry. The exact nature of this chemistry can be sorted out and understood by applying standard analytical techniques. Addition, abstraction, and substitution processes occurring in the main polymer chain appear as changes in the infrared spectrum of irradiated samples. Increases or decreases in the average molecular weight of the polymer due to crosslinking or degradation are apparent from changes in retention time during high pressure liquid chromatography. Persistent radicals can be identified by EPR spectroscopy. As mentioned previously, some intermediates produced during proton radiolysis are electronically excited and their identity can be determined from luminescence spectra recorded during the actual irradiation. Finally, UV-visible absorption spectroscopy can give information on the loss or formation of various absorbing chromophores during or after irradiation.

Combining the data collected concerning the chemistry that occurs, the intermediates that are produced, and the kinetics of their interaction should make it possible to formulate models of the interaction of accelerated protons and aromatic polymers.

IV EXPERIMENTAL METHODOLOGY

A. Materials

A variety of polymeric materials were chosen for the initial proton irradiation experiments; these materials ranged from those currently used in space applications to model systems. The samples included:

1) Kapton - a polyimide widely used in thermal control applications on spacecraft;

2) Narmco 5208 epoxy - a tetraglycidyl-diaminodiphenyl methane based thermoset cured with diaminodiphenyl sulfone; this epoxy is currently widely used as a matrix material for fiber reinforced composites in terrestrial applications and is a candidate matrix material for fabrication of large space structures;

3) Udell 1700 polysulfone - a polysulfone of bisphenol A which is a tough, high temperature thermoplastic material identified as a candidate space processable matrix material for fabrication of large space structures;

4) Poly(1-vinylnaphthalene) - a model aromatic polymer system which has been used previously in energetic electron bombardment studies[33];

5) Anthracene doped poly(1-vinylnaphthalene) - a model material utilized previously in energy transfer and radiation stabilization studies with energetic electrons[33]; and

6) Polymethylmethacrylate - a model acrylate polymer.

For the purposes of these experiments, all samples were prepared in film form with thicknesses ranging from 4×10^{-3} - 3×10^{-2} cm. Most samples were on the order of 1×10^{-2} cm (.005 in.) thick. The Kapton was purchased in thin sheets

and used as received, the PMMA and polysulfone were compression molded (without use of mold release agents), the epoxy was cured in film form and the PlVN films were solvent cast from methylene chloride and extensively dried prior to use. A summary of relevant properties of materials utilized in this study is given in Table I.

B. Irradiation

1. Sample Chamber

All samples were irradiated at room temperature in vacuum ($\leq 10^{-4}$ N/m^2) with 3 MeV protons from a Tandem Van de Graff Accelerator at the Kellogg Radiation Laboratory of the California Institute of Technology. The proton beam was confined in an evacuated steel pipe with a 10 cm internal diameter. The sample chamber was a short section of this pipe which could be isolated from the vacuum system to allow sample mounting and removal. Most polymer film samples were mounted on a brass plate which was 11 cm x 3.5 cm x 0.3 cm and held in place with metal clips. Three samples, ~ 2 cm x 2 cm, could be mounted simultaneously, each being placed over a 1.1 cm diameter hole in the plate to allow measurement of transmitted beam current with a Faraday cup located behind the sample holder. The brass plate was bolted to a copper rod of ~ 1.5 cm diameter which extended out of the sample chamber through a vacuum O-ring assembly. This rod could be pushed in or retracted to selectively irradiate individual samples or to allow the beam to pass completely beyond the sample holder for incident beam current measurements. The spot size of the beam at the samples was ~ 2 cm diameter. A quartz window was located on the opposite side of the chamber from the sample holder to allow viewing of the samples and collection of visible and UV emission during irradiation. Schematic drawings of the sample chamber and holder are shown in Figure 1.

Table I. Relevant Properties of Polymeric Materials Utilized in Energetic Proton Bombardment Studies

Material	Composition	Molecular Weight (g/mole)	Density (g/cm^3)	Tg (°C)	Specific Heat (J/g-°C)	Film Thickness (cm)
Kapton	$C_{22}H_{10}N_2O_5$	---	1.42	400	1.09	.013
Polysulfone	$C_{27}H_{22}O_4S$	30,000	1.24	185	1.25	.013
Epoxy	$C_{25}H_{30}N_2O_4$ (75%) $C_{12}H_{12}N_2O_2S$ (25%)	---	1.27	200	1.05	.004 .009 .030
PMMA	$C_5H_8O_2$	250,000	1.20	95	1.46	.014
PIVN	$C_{12}H_{10}$	150,000	1.2	160	1.2	.010

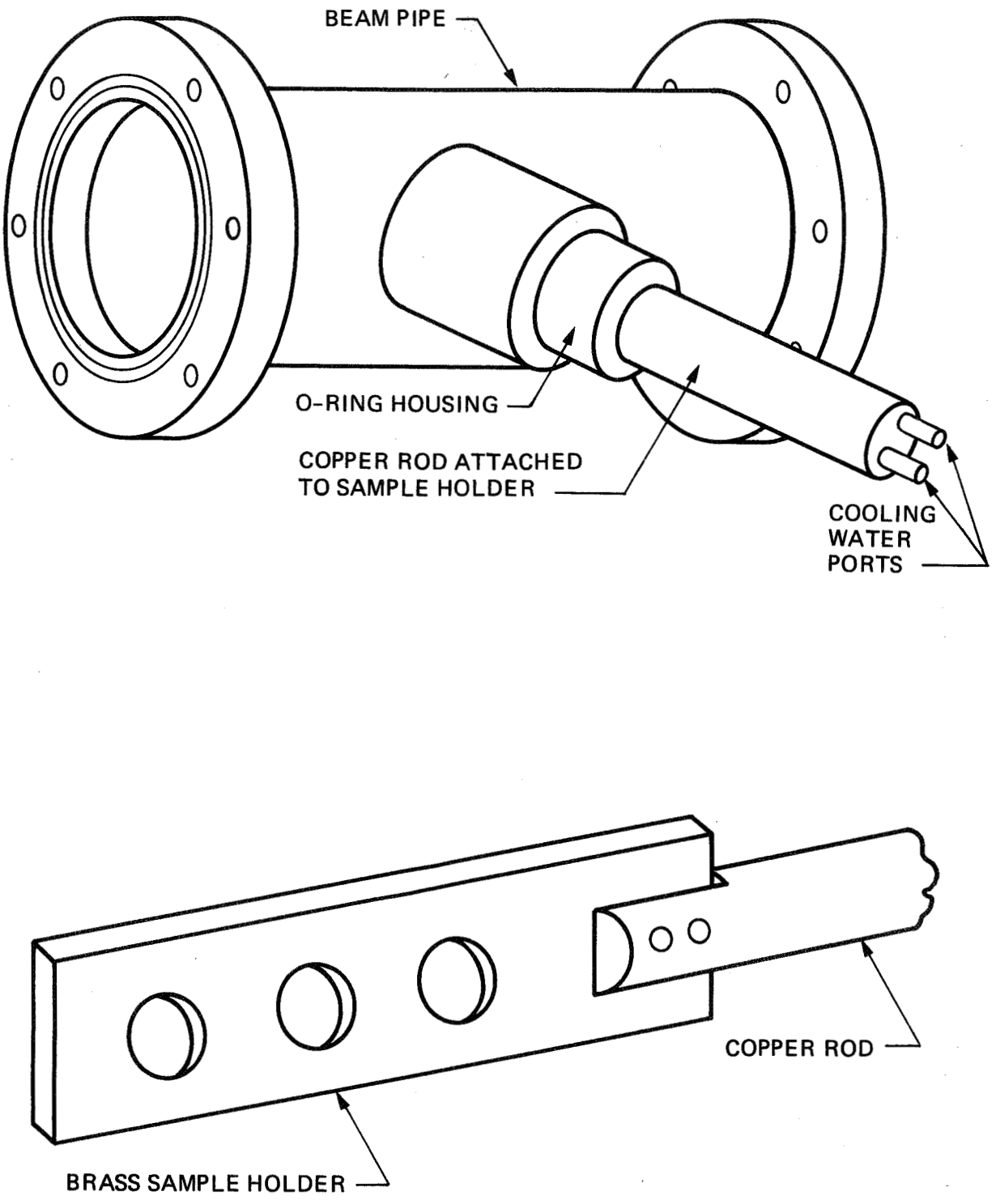

Figure 1. Schematic Drawing of Sample Chamber and Holder Utilized in Proton Bombardment Studies

2. Beam Energy

Protons of energy from almost zero to hundreds of MeVs are found in the space environment. For this initial study, however, it was decided to work with only a single beam energy. In choosing an energy, two issues were given primary consideration. First, in order to obtain the maximum absorbed dose with reasonable uniformity through the sample, it was desirable to choose an energy such that the protons approximately penetrated the sample thickness, which in most cases was ~ $1x10^{-2}$ cm. From data on stopping power and target depth of protons in matter, it can be seen that hydrocarbon solids behave, to a good approximation, as carbon. Ignoring the few heavier nuclei present in the irradiated samples (N,O,S), and using this approximation, the target depth of protons in the film samples can be estimated as a function of energy and density.[34] These results are given in Table II. Examination of the target depths given in Table II shows that an energy of at least 3 MeV is required to meet the first criteria. The second consideration in choosing a beam energy was that the threshold for neutron generation by protons in carbon is 3.2 MeV. In order to avoid potential radiation hazards, it was decided not to exceed this threshold energy and thus a value of 3 MeV for the proton energy was selected.

3. Beam Current

The rate at which dose is accumulated is determined by the magnitude of the proton beam current. Since time on the accelerator was limited, it was desirable to maximize the rate of energy input while at the same time keeping thermal effects to a minimum. Obviously there is a trade-off to be made between accumulated dose, reasonable irradiation time, and allowable temperature rise in the samples. Given the desired dose levels and the constraints of time, it was determined that temperature increases of ~ 10 K

Table II. Estimated Target Depths of Protons in Polymers as a Function of Energy and Density

Proton Energy (MeV)	Target Depth (cm)		
	$\rho = 1.2$	$\rho = 1.3$	$\rho = 1.4$
1	2.45×10^{-3}	2.26×10^{-3}	2.10×10^{-3}
2	6.97×10^{-3}	6.43×10^{-3}	5.97×10^{-3}
3	1.36×10^{-2}	1.26×10^{-2}	1.17×10^{-2}
4	2.09×10^{-2}	1.93×10^{-2}	1.79×10^{-2}
5	3.60×10^{-2}	3.33×10^{-2}	3.09×10^{-2}

were acceptable. The temperature rise in a sample is determined by the rate at which energy is deposited by absorption of the proton beam and the rate at which heat is dissipated to the environment. Two mechanisms of heat dissipation, conduction and radiation, have been considered.

Polymer films were mounted on metal sample supports as discussed in section II.B.1. Conduction of heat away through these supports was the primary mechanism of heat dissipation. The expected temperature rise in the polymer samples as a function of the rate of energy absorption can be estimated from heat transport theory. The sample holder can be modeled as insulated rods conducting heat from a hot reservoir (sample) to a cool one (the laboratory). A schematic representation of such a system is shown in Figure 2. The polymer sample (P), upon which the proton beam is incident is assumed to be in good thermal contact with a brass rod (B) of cross sectional area 1.05 cm^2 which in turn is assumed to be in good thermal contact with a copper rod (C) of cross sectional area 1.77 cm^2. The temperatures T_0, T_1, and T_2 are the temperatures in the lab, at the brass/copper interface and at the sample respectively. The rate of heat transfer, dq/dt, along a rod of cross sectional area A and length L is given by the expression

$$\frac{dq}{dt} = kA \frac{T_{hot} - T_{cool}}{L} \qquad (1)$$

where k is the thermal conductivity of the rod material (1.09 and 3.85 J/s-cm-K for brass and copper respectively). Using equation 1, the rates of heat transfer in the brass and copper rods can be written as:

$$\left(\frac{dq}{dt}\right)_{brass} = 0.23\ (T_2-T_1) \qquad (2a)$$

$$\left(\frac{dq}{dt}\right)_{copper} = 0.34\ (T_1-T_0) \qquad (2b)$$

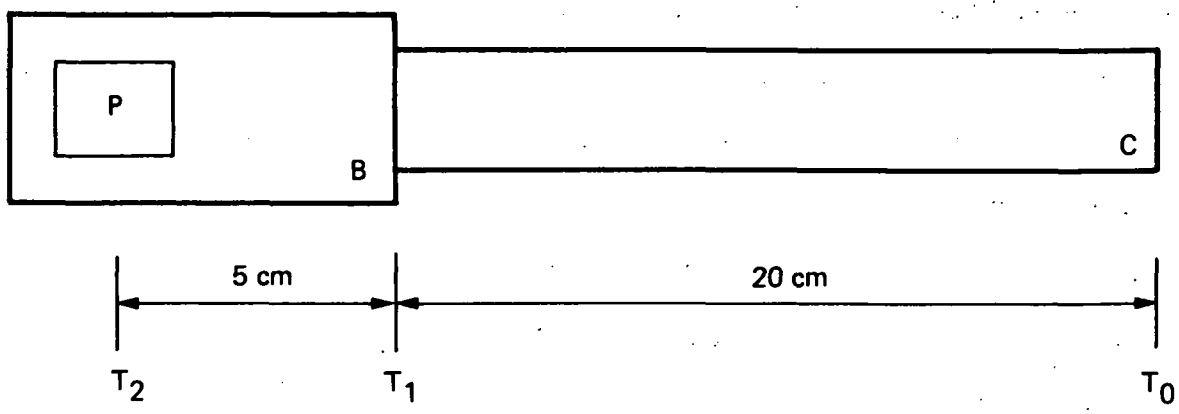

Figure 2. Schematic Representation of Sample Mount Used in Estimation of the Rate of Heat Dissipation During Proton Bombardment of Polymer Films. The polymer sample, brass sample holder and copper rod are designated P, B and C respectively.

At equilibrium, the heat flow in the system is described by a single value and thus

$$\left(\frac{dq}{dt}\right)_{brass} = \left(\frac{dq}{dt}\right)_{copper} = \left(\frac{dQ}{dt}\right) \qquad (3)$$

Letting T_0 = 300 K, the value of dQ/dt corresponding to a 10 K rise in temperature (T_2 = 310 K) can be estimated from equations 2 and 3 to be ~ 1.4 J/s. This is equivalent to ~ 500 nA of 3 MeV protons or ~ 150 nA/cm^2 proton beam current.

The calculation described above is of course very simplified since, for example, thermal contacts are assumed to be perfect and heat conduction in the films is ignored. A major concern is the fact that a portion of the films near the center of the beam are not in any contact with the metal where the holes have been drilled in the sample holder. Heat dissipation in this region is aided to some extent by radiation from the film surfaces; this process is quite efficient due to the relatively high emissivity (ε = 0.9) for most organic polymers.

Taking into account the uncertainties in estimating heat dissipation efficiency, beam currents in the vast majority of cases were held to <75 nA/cm^2 (~ 1 Mrad/s) in order to guard against overheating the samples. There was no evidence of enhanced degradation in the middle of the samples (with the possible exception of PMMA) due to hot spot formation where the films were not in contact with the metal. Furthermore, the estimated temperature rise is consistent with thermocouple[35] and infrared emission[36] measurements made on polymers during electron irradiation at comparable dose rates. If the issue of temperature increases in the samples were to become very important, better thermal control could be obtained by using a solid copper sample holder with external cooling.

4. Beam Uniformity

Under normal operating conditions, the proton beam energy and current are established and then the beam is focused to a small spot (0.5 - 0.01 cm^2) on the sample. Indeed, in these experiments, once the beam was properly stabilized, there was negligible variation in particle energy and current. However, in the case of the polymer films, it was desirable to defocus the beam in order to achieve a reasonably uniform dose over an area of ~ 5 cm^2. To disperse the beam, a thin Ni scattering foil was placed upstream of the samples.

The theory of multiple scattering of medium energy protons has been worked out by Marion and Zimmerman.[37] They have shown that scattering by a metal foil produces an axially symmetric distribution downstream which is approximately Gaussian. The angular distribution can be written as

$$I(\theta) = I(0) \exp(-\theta^2/\theta_e^2) \qquad (4)$$

where $I(0)$ is the beam intensity on axis, $I(\theta)$ is the beam intensity off axis at angle θ and θ_e is the angle at which the beam intensity has fallen to 1/e

of its on axis value. ϵ_ϵ can be calculated from the properties of the foil and the incident particles.[37] For a 10000Å thick Ni foil and 3 MeV protons, θ_e is calculated to be .0195 radians. The fraction of the beam stopped by the foil is negligible. The stopping power of Ni for 3 MeV protons is 6.5×10^{-15} eV/(atoms/cm^2). Assuming a 10000Å thick Ni foil of density 8.9 g/cm^3, the energy loss is 0.06 MeV or less than 2%.

The geometry of the sample relative to the scattering foil is shown in Figure 3.

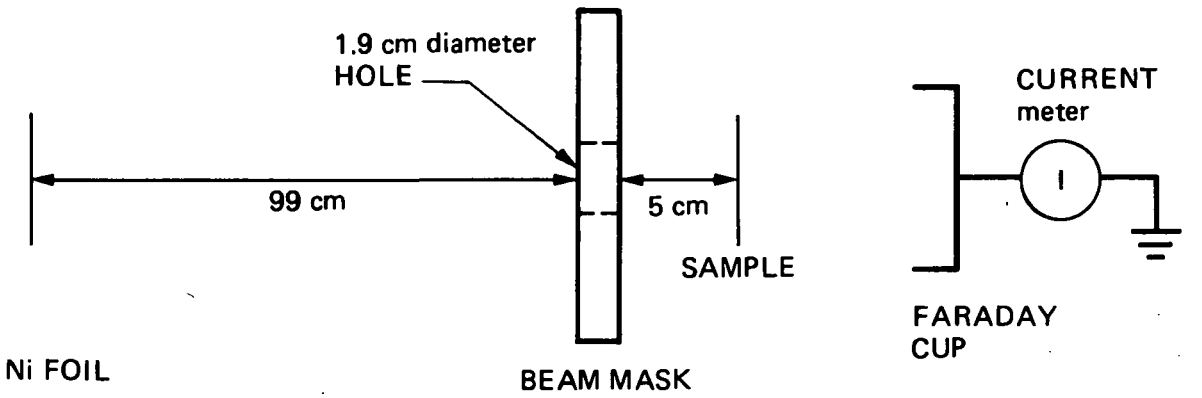

Figure 3. Schematic Drawing Showing Position of the Sample Relative to the Ni Scattering Foil, Beam Mask and Faraday Cup

The foil is 99 cm upstream of a mask which blocks all but the central portion of the beam. The sample sits 5 cm behind the mask. The irradiated portion of the sample is then a circle of diameter 1.9 cm. The edge of the circle corresponds to an angle of

$$\theta = \tan^{-1}\left(\frac{0.5 \times 1.9}{104}\right) = 0.0091 \text{ radians} \qquad (5)$$

Substituting this value into equation 4 indicates that at the edge of the irradiated spot on the films, $I/I_0 = 0.8$, or that in the ideal case, the variation across the irradiated spot is only 20%. In practice, this deviation is probably less due to time dependent geometric fluctuations in the beam which tend to average everything out.

The fraction of the beam that is transmitted by the Ni foil and that actually reaches the sample, F, can be calculated by the expression

$$F = \frac{\int_0^{0.0091} \exp\left(-\theta^2/\theta_e^2\right) d\theta}{\int_0^{\pi} \exp\left(-\theta^2/\theta_e^2\right) d\theta} \tag{6}$$

If the following substitutions are made

$$x = \theta/\theta_e = 51.3\theta$$
$$x^2 = \theta^2/\theta_e^2$$
$$dx = 1/\theta_e \cdot d\theta$$

then equation 6 can be written in the familiar form of the Gaussian error function

$$F = \frac{\int_0^{0.468} e^{-x^2} dx}{\int_0^{161} e^{-x^2} dx} \tag{7}$$

Evaluation of the integrals in equation 7 gives a value of 0.49, or approximately one half of the transmitted beam eventually reaches the sample.

In a few cases, samples were actually mounted on the surface of the mask facing the Ni foil in order to get a continuous distribution of doses along a radius extending out from the axis of the beam. The dose in a small area, dA, was calculated by integrating equation 4 over the appropriate limits using polar coordinates. Comparison tests on samples exposed in this manner were in good agreement with the results from samples mounted on the sample holder.

5. Irradiation Conditions

A total of 41 samples were irradiated in this study under widely varying conditions depending on the radiation sensitivity of the specific materials. Maximum and minimum values of various parameters are given in Table III.

Dose rates and accumulated total dose were calculated for each sample based on beam current measurements. In almost all cases, one hole (1.1 cm diameter) in the sample holder was left uncovered and used to measure beam current before and after irradiation. A sample calculation of dose is given below for an actual PMMA film exposed in the experiments:

- total beam current measured through 1.1 cm diameter hole = 70 nA

$$\text{thus} \quad \frac{\text{current}}{\text{area}} = \frac{70 \text{ nA}}{\pi \cdot (0.55)^2} = 74 \text{ nA/cm}^2$$

- the rate of proton bombardment is then

$$\frac{74\times10^{-9} \text{ coulombs}}{\text{cm}^2\text{-s}} \cdot \frac{1}{1.6\times10^{-19} \text{ coulombs/proton}} = 4.6\times10^{11} \frac{\text{protons}}{\text{cm}^2\text{-s}}$$

- the incident power is then

$$\frac{4.6\times10^{11} \text{ protons}}{\text{cm}^2\text{-s}} \cdot \frac{3 \text{ MeV}}{\text{proton}} \cdot \frac{1.6\times10^{-6} \text{ erg}}{\text{MeV}} = 2.2\times10^{6} \frac{\text{erg}}{\text{cm}^2\text{-s}}$$

- the film thickness was 1.4×10^{-2} cm and the target depth for 3 MeV protons in PMMA is ~ 1.35×10^{-2} cm; thus total absorption is assumed (transmitted beam currents were negligible)

Table III. Range of Operating Parameters Used in Proton Bombardment Studies

Parameter	Units	Minimum	Maximum
radiation time	minutes	3	230
beam current	nA/cm^2	8.5	158
dose rate	Mrad/s	0.15	2.6
accumulated dose	Mrad	48	10110

- the unit of dose is the rad which equals 100 ergs of radiation absorbed per gram of material. Thus, the dose rate is

$$\frac{\text{dose}}{\text{time}} = \frac{2.2\text{x}10^{6}\ \text{ergs}}{\text{cm}^{2}\text{-s}} \cdot \frac{1}{1.4\text{x}10^{-2}\text{cm}} \cdot \frac{1\ \text{cm}^{3}}{1.2\ \text{g}} \cdot \frac{1\ \text{rad}}{100\ \text{ergs/g}}$$

$$= 1.32\text{X}10^{6}\ \text{rad/s}$$

$$= 1.32\ \text{Mrad/s}$$

- the radiation time of this sample was 14 minutes and thus the total dose is

$$1.32\ \text{Mrad/s} \cdot 840\ \text{s} = 1109\ \text{Mrad}$$

C. Analysis

A variety of analytical techniques were applied to irradiated samples. Generally, materials were investigated first for changes in molecular weight (crosslinking or chain scission) then for changes in mechanical properties (modulus, T_g, etc.) and finally for spectroscopic changes indicative of chemical alteration due to the proton beam. Obviously not all tests were run on all samples. In some cases, the condition of the irradiated material precluded running a specific test. A brief description of the analytical techniques employed is given below.

Sol-gel studies were carried out on films extracted with methylene chloride. Molecular weight distributions in the soluble fraction were recorded on a Waters 6000 Modular High Pressure Liquid Chromatograph (HPLC) equipped with microstyragel columns (10, 10^2, 10^3, 10^4, Å pores). Narrow molecular weight distribution polystyrene was used as a standard for calibration. A Hewlett Packard Model 8450A rapid scanning UV-visible absorption spectrometer

was utilized in tandem with the HPLC in order to get spectra of individual fractions as they exited the columns.

Tensile modulus data were recorded on a temperature controlled Rheovibron operated in a static mode. Dynamic viscoelastic measurements were made on a Dupont 1090 DMA apparatus. Infrared spectra of irradiated films were recorded on a Digilab FTIR spectrometer operated in attenuated total reflectance mode. Spectra of the soluble fractions were recorded in the diffuse reflectance mode following their extraction with methylene chloride and deposition on KCl powder. Free radical species were monitored by electron spin resonance spectroscopy using a Varian Century Series E-15 ESR spectrometer. Electronic absorption spectra were recorded on a Cary 219 spectrometer and postirradiation fluorescence studies were performed on a Perkin-Elmer MPF-3 fluorescence spectrophotometer. In-situ emission spectra were recorded during actual irradiation through the quartz window. Emitted light was collected and dispersed by a .25 m Jobin-Yvon monochromator and detected with a RCA 1P28 photomultiplier tube. Resolution was ~2 nm.

V RESULTS AND DISCUSSION

A. Polysulfone

Udell 1700 polysulfone has the chemical structure shown below.

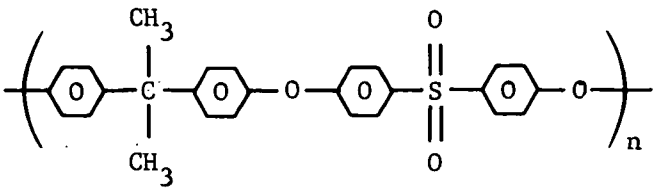

Because of its processability, its well characterized structure, and its relevance to actual space applications, this material was selected to be the most extensively investigated.[30] Consequently, a large portion of the experimental section is devoted to this material and in general, the analysis of the irradiated polysulfone can serve as a model for analysis of the effects of proton irradiation on almost any polymeric material.

1. Sol-Gel Studies

Proton irradiation of polysulfone results in both the fracture of single polymer macromolecules (chain scission) and the fusion of two or more polymer macromolecules (crosslinking). Sol-gel studies on irradiated films show that the initial formation of insoluble material occurs at doses somewhere between 250 Mrad and 600 Mrad. The fraction of insoluble material increases with dosage. Results of sol-gel measurements on six typical samples as a function of dose are given in Table IV. The molecular weight distributions in the soluble fractions have been determined by high pressure liquid chromatography. Chromatograms of material extracted from irradiated samples are shown in Figure 4. The calculated number average and weight average molecular weights are listed in Table V. The molecular weights in the soluble fractions drop as a function of dose. The structure apparent at low molecular weight (even in the control sample) arises from the presence of oligomeric species of order n = 3-6.

Table IV. Results of Sol-Gel Measurements on Proton Irradiated Polysulfone

Sample No.	Dose (Mrad)	Soluble Fraction
0	0	1.0
1	672	0.592
2	1285	0.284
3	2281	0.212
4	3427	0.167
5	4680	0.149

A measure of the crosslinking and chain scission yields can be obtained from the sol-gel data. Charlesby and Pinner[38] have shown that the change in soluble fraction (S) of a polymer as a function of radiation dose (r) is given by the expression

$$(S + S^{1/2}) = 1/q_o N_o r + p_o/q_o \tag{8}$$

In equation (8), p_o is the fraction of polymer chains undergoing scission per unit dose, q_o is the fraction of chains undergoing crosslinking per unit dose and N_o is the initial number average degree of polymerization given by

$$N_o = \bar{M}_n/w \tag{9}$$

where w is the molecular weight of the repeating unit. If the dose is given in Mrad, then the expressions for the radiation yields of crosslinking and chain scission are[39]

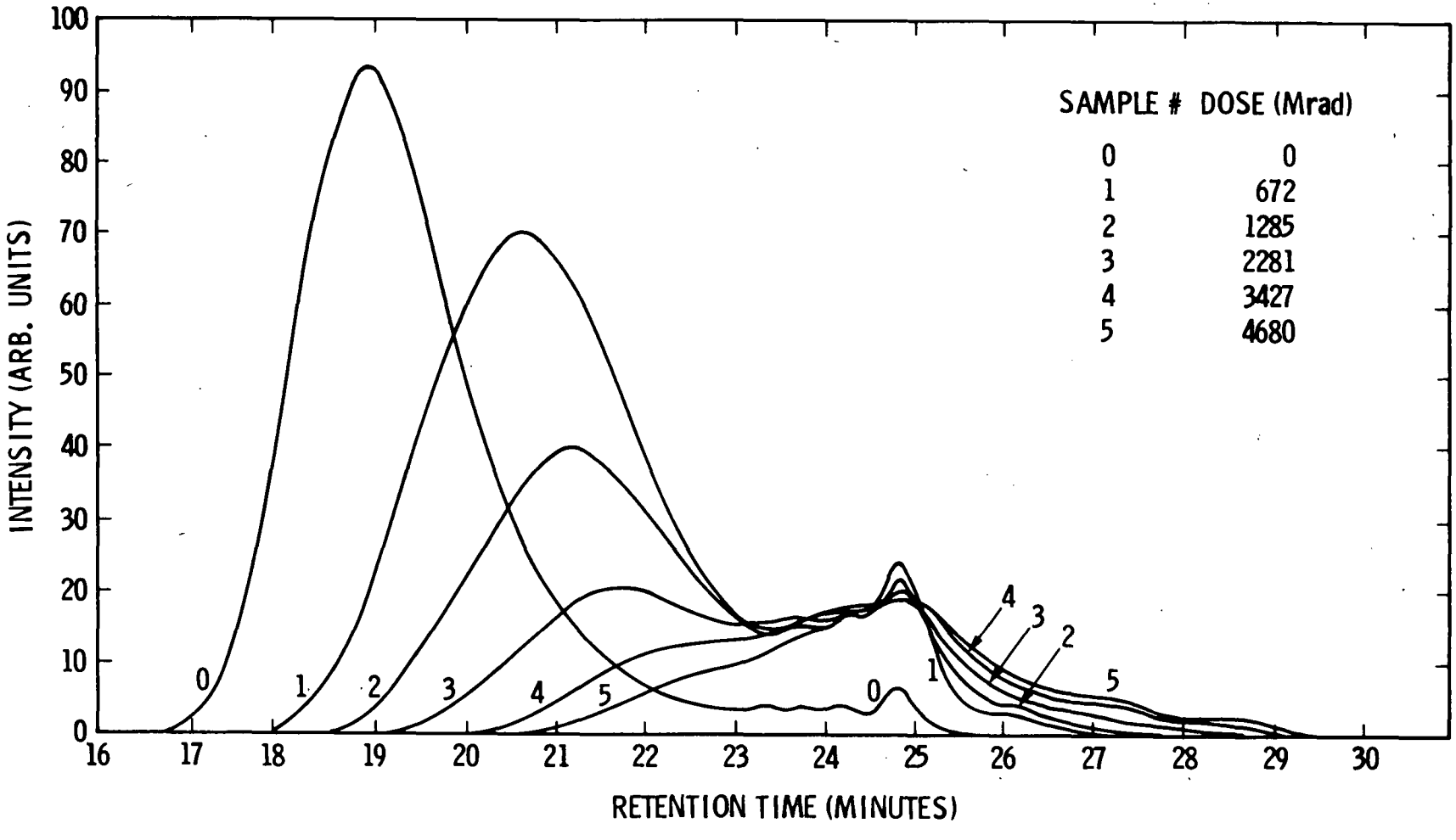

Figure 4. Chromatograms of Soluble Fractions of Proton Irradiated Polysulfone

Table V. Molecular Weight Data on Proton Irradiated Polysulfone Extract

Sample Number	Dose (Mrad)	$\bar{M}n$	$\bar{M}w$	$\bar{M}w/\bar{M}n$
0	0	46000	71600	1.56
1	672	5889	10605	1.80
2	1285	4309	7771	1.80
3	2281	2739	5026	1.83
4	3427	2227	3213	1.44
5	4680	1793	2650	1.48

$$G_{\text{chain scission}} = 9.6 \times 10^5 \, p_o/w \qquad (10a)$$

$$G_{\text{crosslink}} = 4.8 \times 10^5 \, q_o/w \qquad (10b)$$

A Charlesby-Pinner plot of the sol-gel data is shown in Figure 5. From the slope and the intercept, p_o and q_o are calculated to be 5.69×10^{-6} Mrad^{-1} and 1.50×10^{-5} Mrad^{-1} respectively. Using expressions (10a) and (10b), the G values for crosslinking and chain scission are calculated to be

$$G_{\text{crosslink}} = 0.016$$

$$G_{\text{chain scission}} = 0.012$$

The radiation induced gel point is the point where the line in Figure 5 intersects $S+S^{1/2} = 2$. This corresponds to a gel dose (r_{gel}) of 396 Mrad which is consistent with our observation that insoluble material is present in all samples receiving doses of more than several hundred Mrad. Charlesby[39] has shown that $G_{\text{crosslink}}$ may be related to $\bar{M}_w$ by the following expression:

$$G_{\text{crosslink}} = 4.8 \times 10^5 \, / \, r_{gel}\bar{M}_w \qquad (11)$$

Substitution of r_{gel} into equation (11) gives $G_{\text{crosslink}} = 0.017$ which agrees well with that calculated from the slope of the Charlesby-Pinner plot.

2. Physical and Mechanical Property Measurements

Polysulfone samples receiving high doses of proton radiation show considerable embrittlement making them difficult to handle. Stress-strain data have been recorded on several samples of relatively low dose and typical data recorded at 100°C are presented in Figure 6. It is seen that the tensile modulus increases with increasing dose which is consistent with the observation of embrittlement.

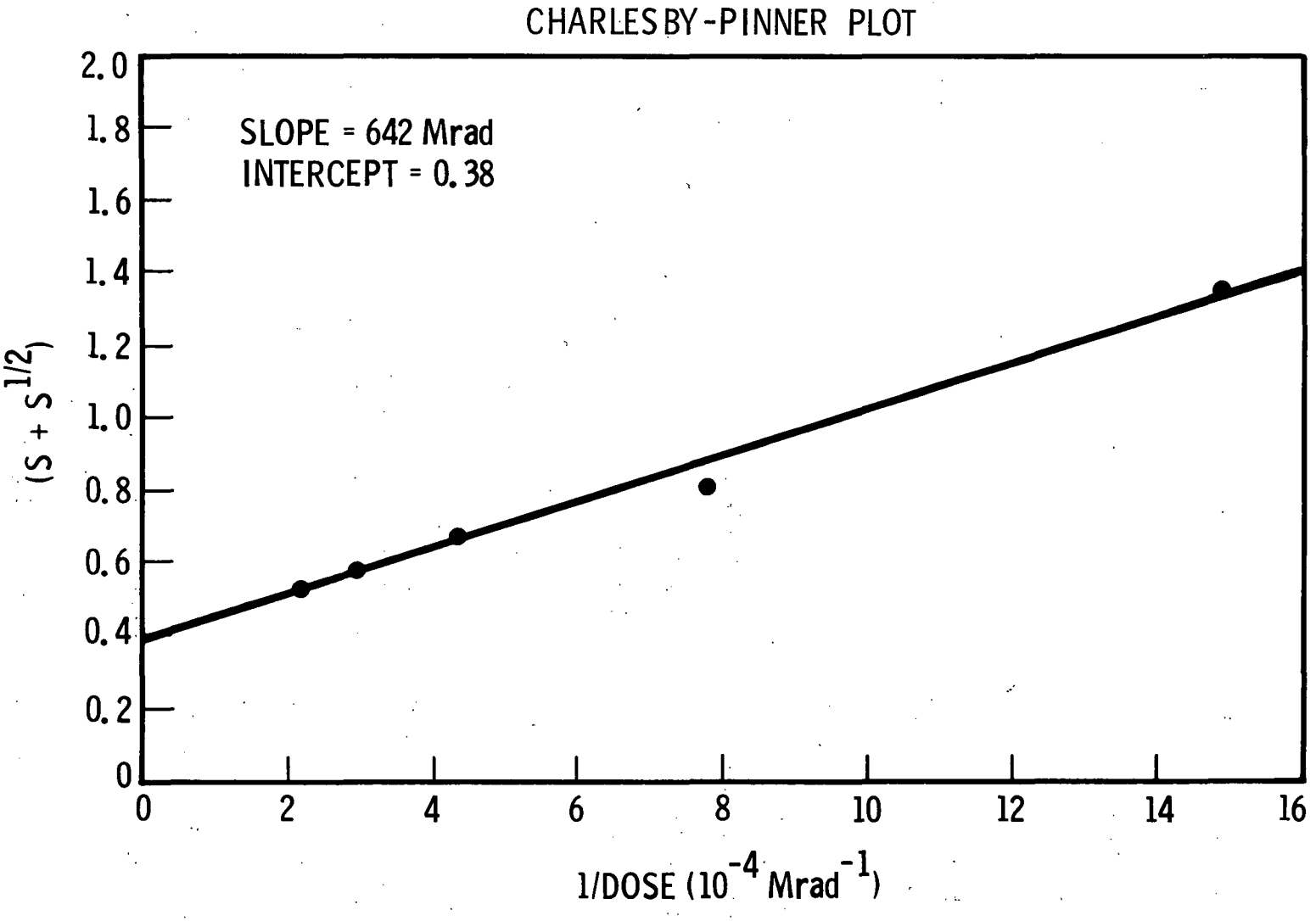

Figure 5. Charlesby-Pinner Plot for Proton Irradiated Polysulfone

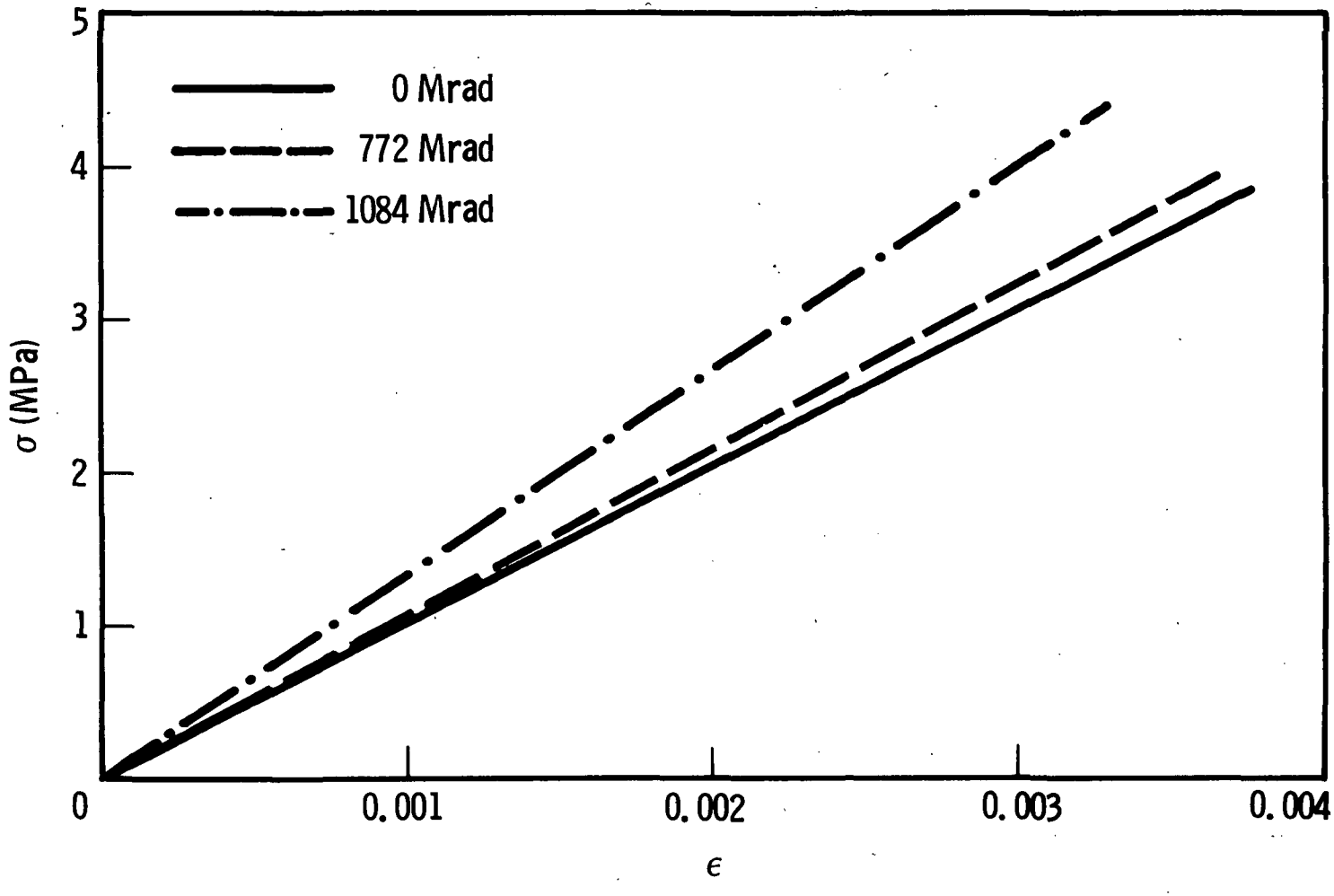

Figure 6. Plot of Stress-Strain Data for Proton Irradiated Polysulfone Recorded at 100°C Showing Increase in Tensile Modulus With Dose

Dynamic viscoelastic properties of irradiated films have been studied by dynamic mechanical analysis. Due to small sample size, reliable quantitative measures of the storage modulus and loss tangent could not be obtained. The T_g and the γ-relaxation temperature however, can clearly be seen in the plot of frequency (storage modulus) versus temperature shown in Figure 7. These data are consistent with those reported in the literature except that no ß transition was observed at 75°C.[40] The measured T_g increases from ~150°C in the control sample to ~220°C at 1366 Mrad. This finding is again consistent with earlier observatons of embrittlement and increases in the tensile modulus. The γ-relaxation temperature of ~-90°C is seen to be insensitive to irradiation. The damping (tanδ) measurements show essentially the same results except that a weak ß-relaxation peak, which did not change with irradiation, was observed near 50°C.

3. Spectroscopic Studies

a. Fourier Transform Infrared (FTIR) Spectroscopy

FTIR studies have been carried out on proton irradiated polysulfone films and their extracts. Measurements on the films themselves were performed in the attenuated total reflectance (ATR) mode. Figure 8 shows the ATR-FTIR spectra of a typical irradiated film (1366 Mrad) and a control film in the region 400-2000 cm^{-1}. There is essentially no difference in the two spectra in this region. ATR-FTIR may not be an optimum technique for studying damage in irradiated samples because it probes only the first few microns below the surface. The films, however, are far too thick to allow transmission FTIR spectra to be recorded.

In an effort to detect chemical changes resulting from irradiation, exposed films were extracted with methylene chloride and the resulting solutions evaporated on KCl powder. FTIR spectra were then recorded in the diffuse

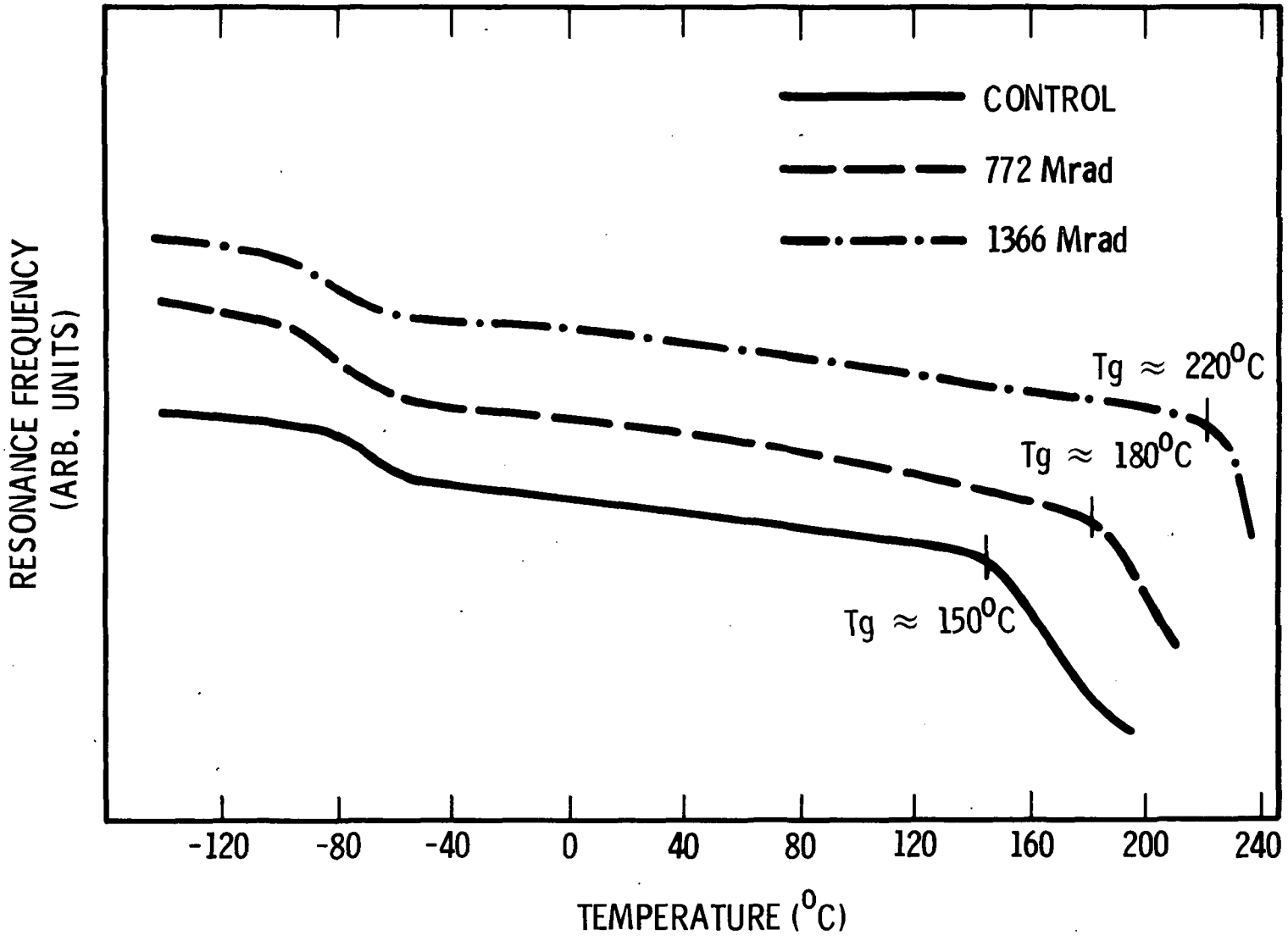

Figure 7. Plot of the Resonance Frequency (Storage Modulus) Versus Temperature as Recorded by DMA for Proton Irradiated Polysulfone Showing T_g and γ-Relaxation Temperatures

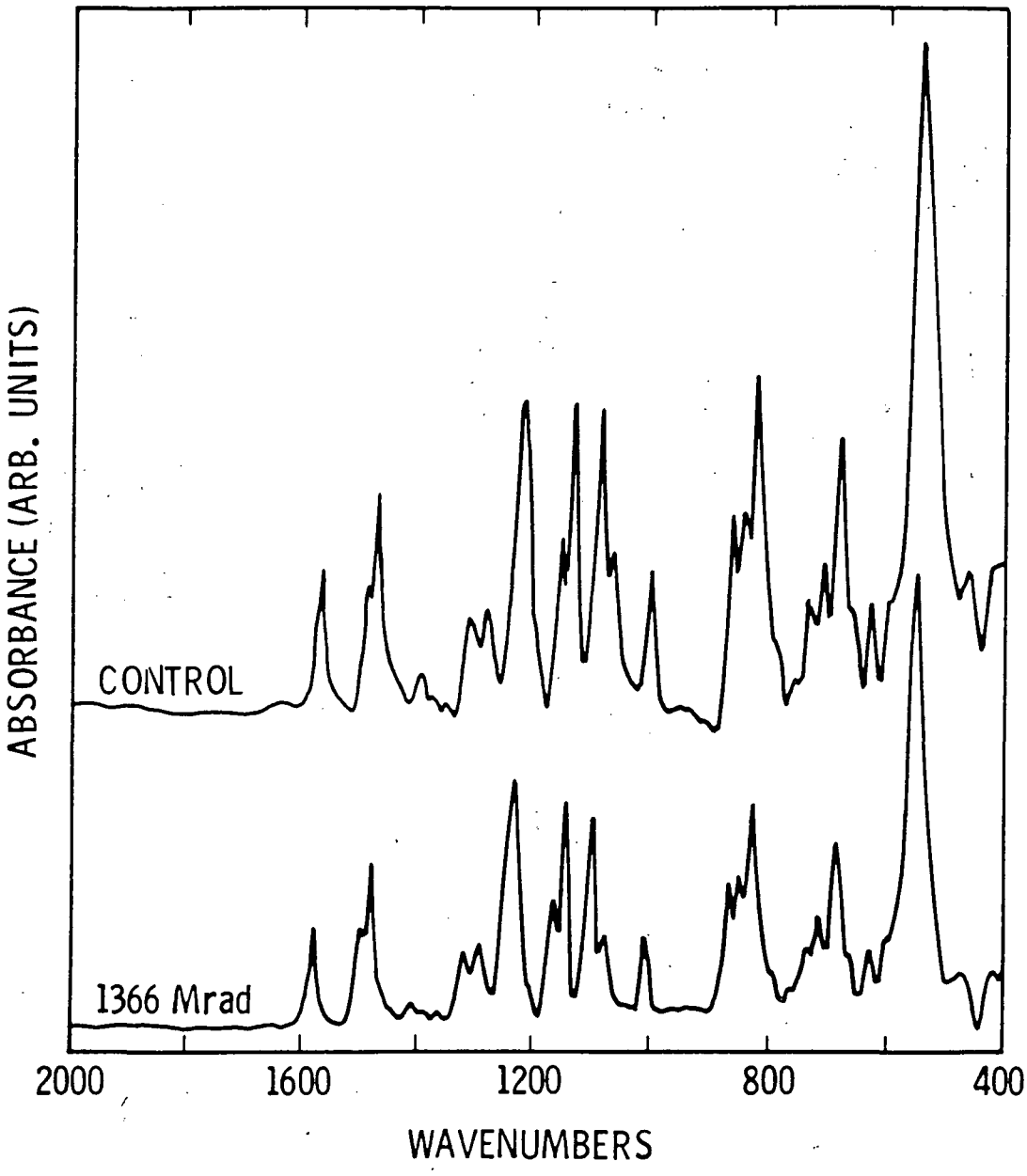

Figure 8. Attenuated Total Reflectance-FTIR Spectra of Control and Proton Irradiated Polysulfone Films

reflectance (DR) mode. Typical DR-FTIR spectra are shown in Figure 9. The most obvious change occurring as a function of dose is the appearance and growth of an -OH absorption band at 3400 cm^{-1}. Other more subtle changes can be observed including a small decrease in bands around 1150 cm^{-1}, 1300 cm^{-1}, and 1400 cm^{-1} which are associated with $-SO_2-$ vibrations[41] and the appearance of features at 1035 cm^{-1} and ~750 cm^{-1} which may be associated with monosubstituted phenyl rings, although this assignment is not certain.

b. Electron Spin Resonance (ESR) Spectroscopy

The ESR spectrum of irradiated polysulfone is shown in Figure 10. This spectrum was recorded ~20 hrs after irradiation (1366 Mrad), during which time the sample was stored at room temperature and exposed to air.

c. Electronic Spectroscopy

The UV-visible absorption spectra of irradiated films were recorded as a function of dose and are shown in Figure 11. The material becomes yellow and the absorption edge moves progressively to the red as dose increases.

In-situ emission spectra were also recorded during the irradiation of films as a function of dose. One set of these spectra is shown in Figure 12. The proton excited emission spectrum of polysulfone appears to show two bands. A short wavelength band with a maximum near 340-350 nm is seen to disappear rapidly as the accumulated dose approaches 300-400 Mrad. A longer wavelength band with a maximum near 380-390 nm appears to be relatively insensitive to dose up to 630 Mrad. UV excitation of films after proton irradiation produces similar emission spectra. At very high proton doses (3000 Mrad) even the long-wavelength emission disappears.

4. Discussion

The results of this study indicate that polysulfone (Udell 1700) is relatively stable to proton bombardment. This generally agrees with

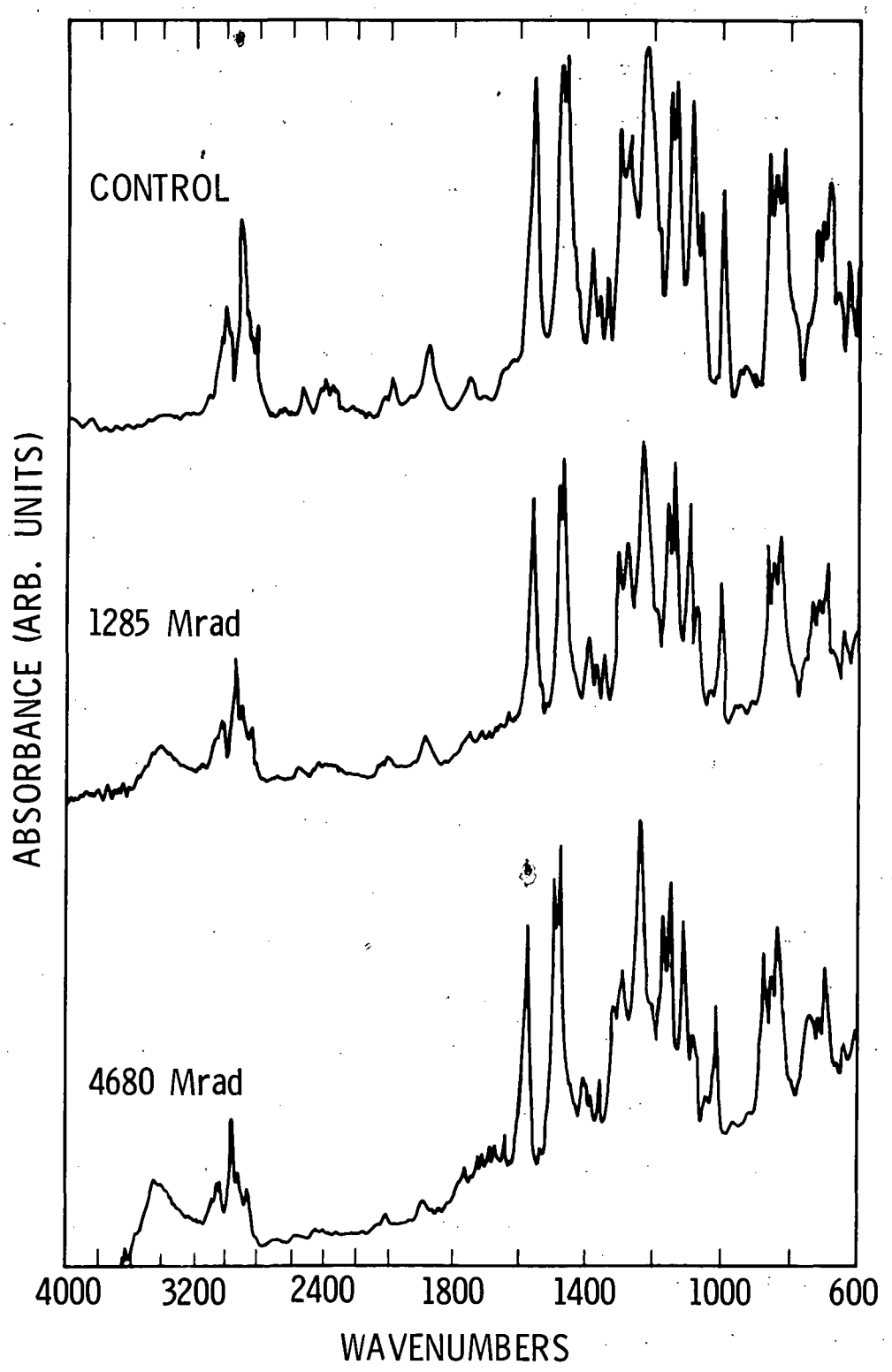

Figure 9. Diffuse Reflectance-FTIR Spectra of Evaporated Sol Fractions (Methylene Chloride Extracted) from Proton Irradiated Polysulfone

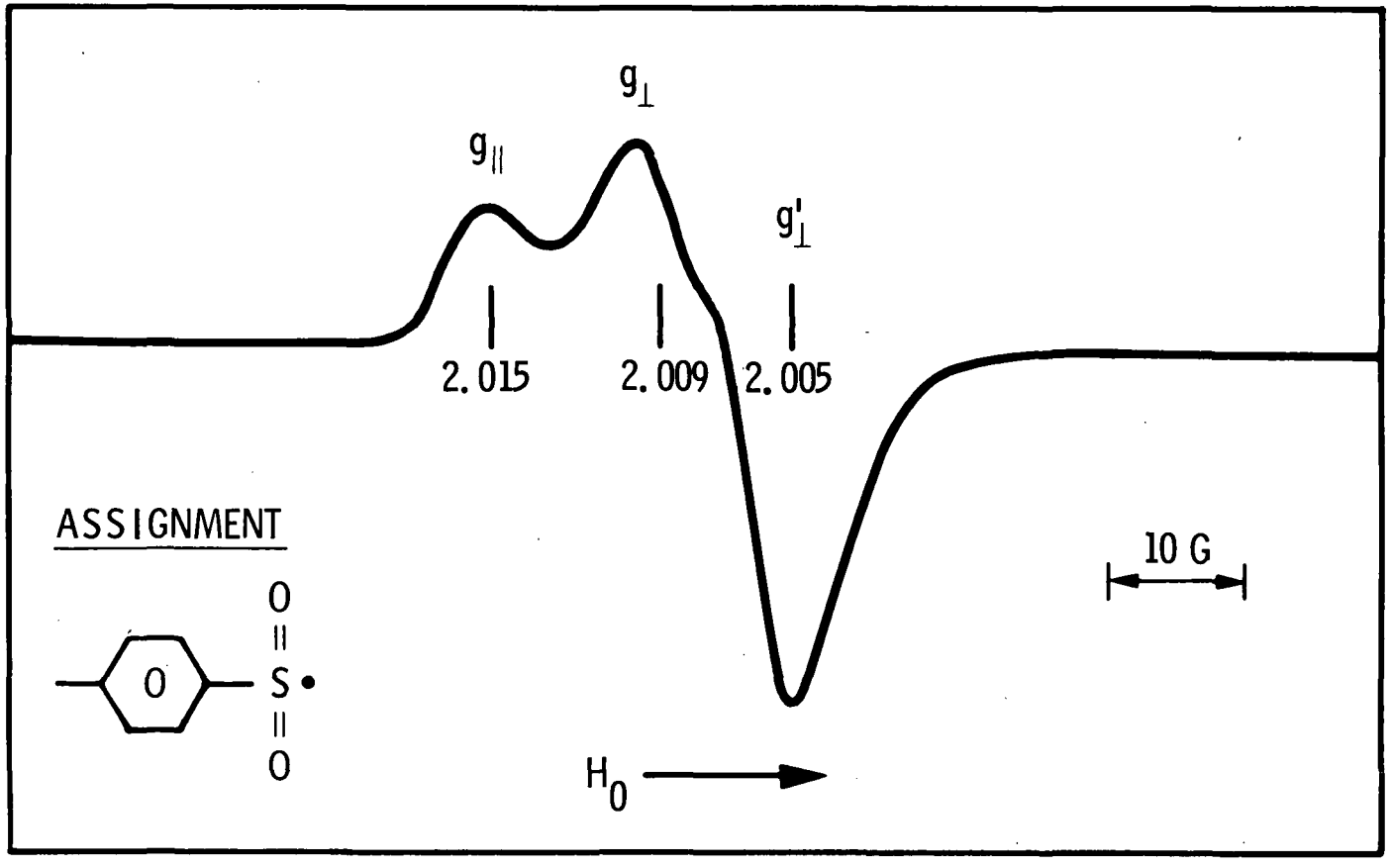

Figure 10. ESR Spectrum of Proton Irradiated Polysulfone

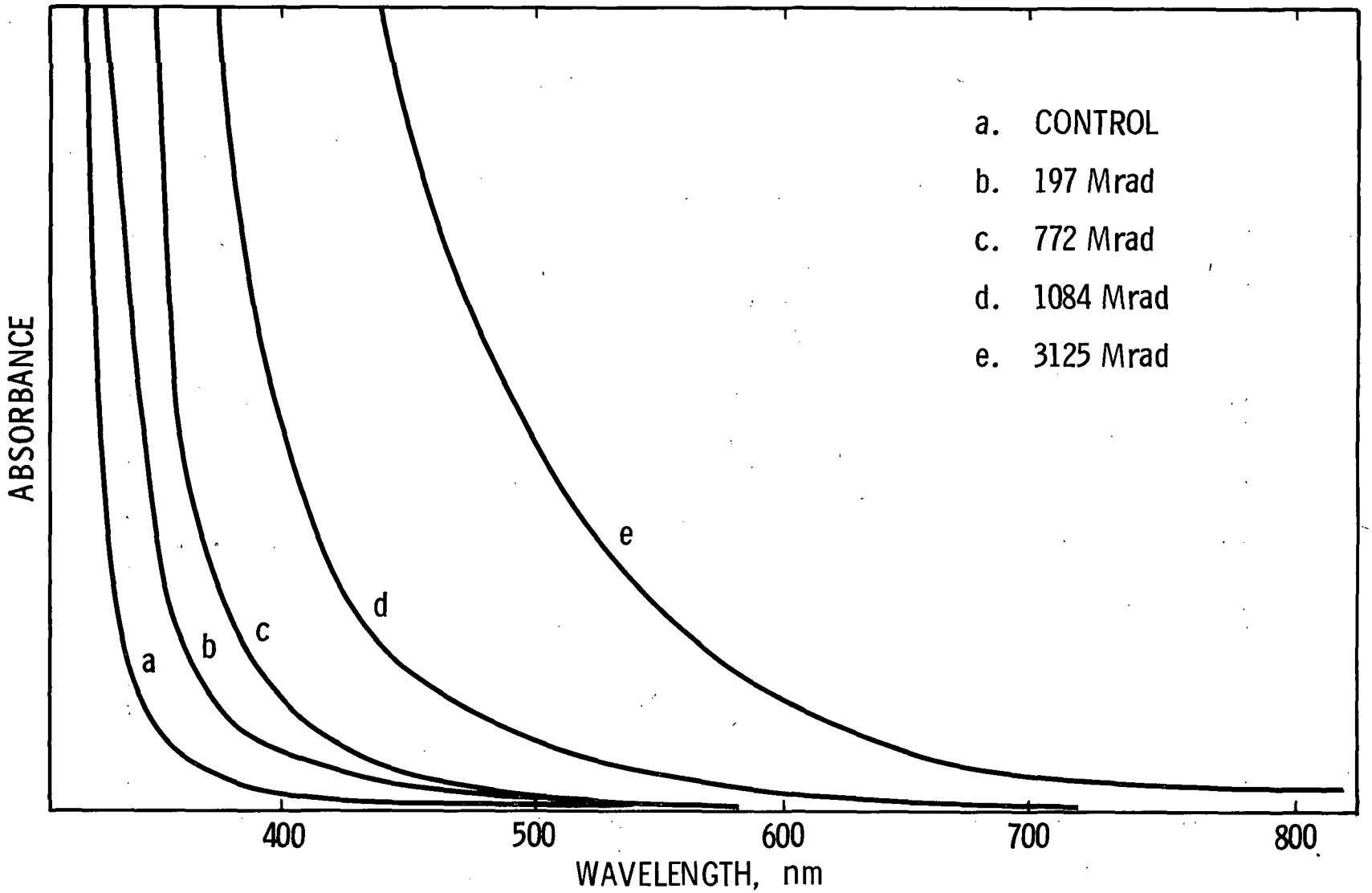

Figure 11. UV-VIS Absorption Spectra of Proton Irradiated Polysulfone as a Function of Dose

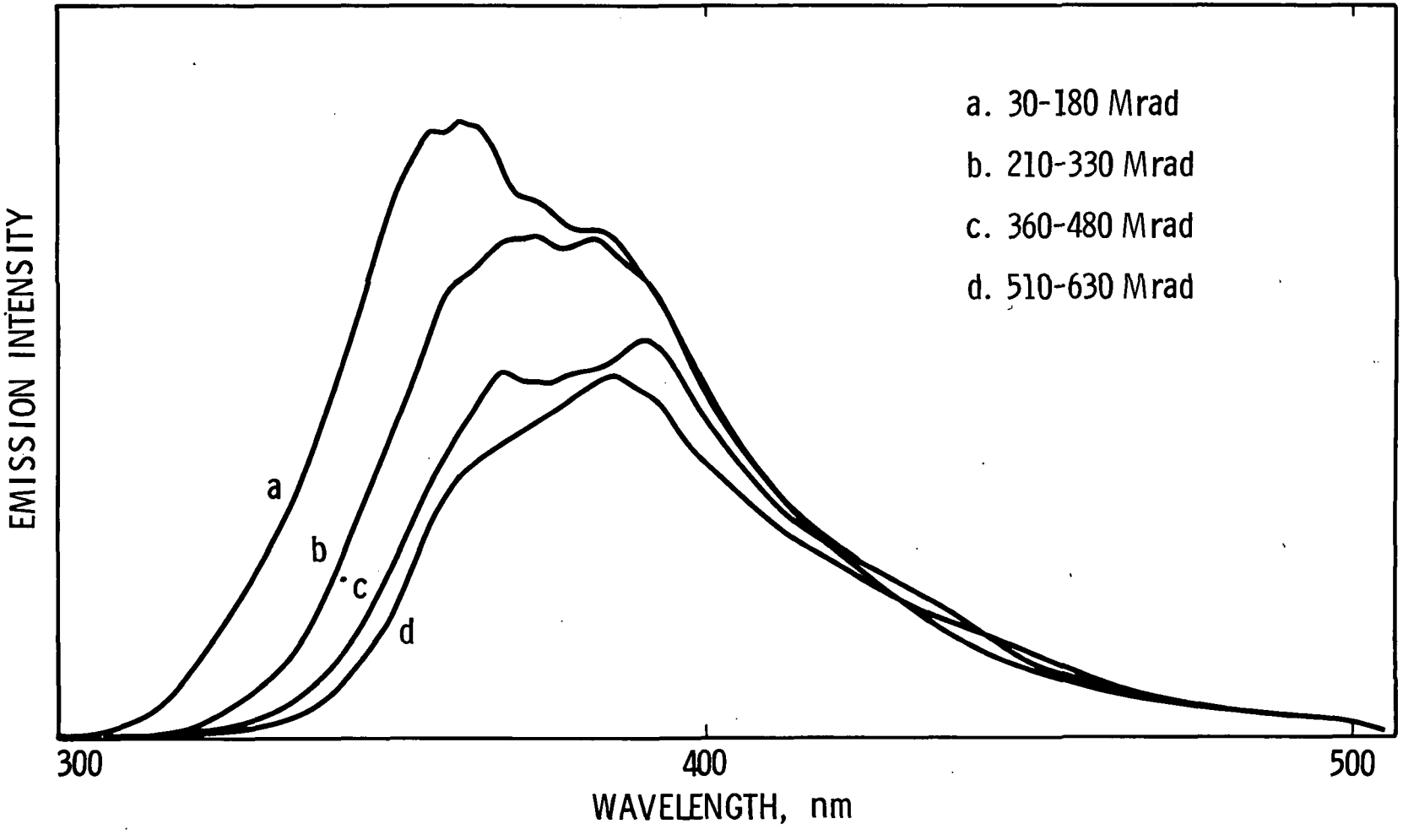

Figure 12. Emission Spectra of Polysulfone Recorded In-situ During Proton Irradiation

results from other exposure studies[41-47] with γ-radiation or electrons, although some specific results differ. It is not surprising that the details of the radiation effects are different with protons since the nature of the particle/matrix interactions are not the same. With the heavier particles, ionization is no longer the only likely initial event. Displacement of the "lattice" atoms due to proton bombardment resulting in broken bonds, non-vertical transitions, and significant local "heating" might be expected to cause much more heterogeneous damage than that observed with electron or γ-irradiation.

Proton bombardment is found to result in both crosslinking and chain scission in polysulfone, as has been previously reported in proton[46], electron[46], and γ-radiation[44] studies. Santos and Sykes[46] have suggested that with electrons and protons, chain scission dominates at low doses while crosslinking dominates at higher dose levels. They report a threshold of 1000 Mrad for crosslinking. No evidence of such a threshold is found in this work. Rather, based on sol-gel studies it appears that both processes occur simultaneously. Crosslinking seems to be occurring from the onset of exposure resulting in initial gel formation near 400 Mrad while chain scission continues to reduce the molecular weight of the soluble fraction even at the highest doses. The radiation yields of $G_{scission}$=.012 and $G_{crosslink}$=.016 measured in this study are in reasonable agreement with the results from γ-radiation studies[44] of $G_{scission}$=.012 and $G_{crosslink}$=0.5. The measured gel dose of ~400 Mrad is also in reasonable agreement with the γ-radiation value of ~250 Mrad.[44] The near equality of scission and crosslinking yields from proton irradiation may be indicative of the more heterogeneous nature of the damage compared to that resulting from γ-radiation.

The crosslinking and chain scission reactions occurring in polysulfone alter the physical and mechanical properties of the material. Irradiated

samples become brittle and show increases in the tensile modulus and T_g. The embrittlement phenomena, probably resulting from crosslinking, is consistent with that observed previously.[44,46]

Earlier proton and electron studies in vacuum[46] found that the modulus showed an initial decrease followed by an increase at higher doses (>5000 Mrad for protons), while electron bombardment in air resulted in the modulus increasing monotonically.[47] γ-radiation exposure produced no change in modulus up to 400 Mrad.[44] The nature of the reported[46] initial drop in modulus (~20%) is not clear. In general, it must be concluded that, at least at higher dose levels, proton and electron bombardment results in an increased tensile modulus in polysulfone.

The glass transition temperature has been reported to drop following proton exposure.[46] With electron bombardment T_g increases with vacuum irradiation[46] and decreases with irradiation in air.[47] We observe a monotonic increase in T_g with dose to a level similar to that observed in electron exposure studies in vacuum.[46] This would seem to be consistent with the embrittlement and modulus increases discussed above.

FTIR studies on polysulfone films showed few if any changes after proton bombardment. The extracted fraction of irradiated films however, did show formation of -OH groups and loss of $-SO_2-$ groups after irradiation. Several authors[41,46] have observed disappearance of $-SO_2-$ bands after irradiation of polysulfones which correlates well with the observation that SO_2 is a major volatile product trapped during γ-irradiation.[44] No other instances of -OH formation have been reported in the literature; however, previous authors have not reported FTIR results above 2000 cm^{-1}.[41,46]

The observed ESR spectrum of irradiated polysulfone is typical of that resulting from randomly oriented radicals with an anisotropic g-tensor in a rigid matrix.[48] The relatively high g-values of the spectrum are indicative

of non-hydrocarbon radicals. It has been suggested[43] that polysulfone irradiated with γ-radiation at low temperature produces phenoxy and aryl-sulfonyl radicals with g values in the range 2.005-2.007. This is consistent with the present observation; however, it is unlikely that phenoxy radicals would have a lifetime of 20 hours, particularly when the sample is exposed to air. Consequently, it is believed that the observed spectrum is probably due to randomly oriented aryl-sulfonyl radicals which might be expected to be more stable at room temperature, as has been found to be the case for alkyl-sulfonyl radicals.[42]

The results of the UV-VIS absorption spectroscopy are similiar to those reported for polysulfone which was γ-irradiated in air and vacuum.[45] For samples irradiated in air, yellowing was probably mainly due to oxidation. In vacuum the yellowing is probably due to generation of species with extended conjugation which causes their excited states to shift to lower energies. Reaction of the samples with oxygen after removal from vacuum, however, cannot be completely ruled out.

The changes in electronic absorption and emission spectra observed on proton irradiation are qualitatively similar to those found in an UV irradiation study.[49] The implications of the absorption and emission data are that initially, there are at least two emissive species present in polysulfone. During the early stages of irradiation new, conjugated, non-emissive species are created whose excited states lie between those of the two emissive species. Formation of these new species leads to the appearance of a longer wavelength absorption feature and quenching of the high energy emitting state with little or no change of the long wavelength emission. As irradiation continues, species with increasingly lower energy excited states are produced, resulting in further red shifts in the absorption spectrum. Ultimately both of the

emissive states are quenched when the energy of the excited states of the product species falls below the energy of the lower emissive state.

The mechanism of damage to polysulfone by protons is probably quite complex. γ-irradiation studies[43,44] have indicated that scission of C-S and C-O bonds in the main chain as shown in equations 12 and 13 are the principal steps in the radiolysis.

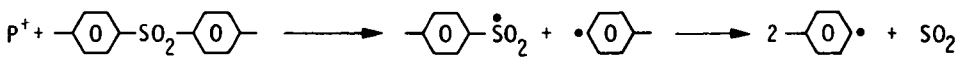

(12)

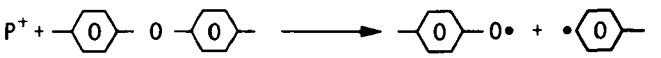

(13)

Observation of the phenyl sulfonyl radical by ESR and the appearance of -OH groups in the FTIR spectra, probably resulting from breaking of the ether linkage followed by hydrogen abstraction (equation 14), suggests that C-O and C-S bond cleavage may also be major damage mechanisms during proton exposure.

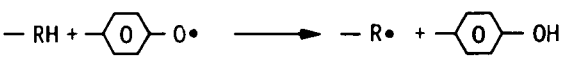

(14)

Loss of SO_2 bands in the FTIR spectra probably indicates that the phenyl-sulfonyl radicals slowly decay by elimination of SO_2, leaving behind a phenyl radical. This is consistent with the results of product analysis in earlier work.[44]

Brown and O'Donnell[44] have shown that the isopropylidene linkage in polysulfone is involved in both chain scission and crosslinking processes. It is

possible that it is primarily the methyl protons that are abstracted by phenyl and phenoxy radicals leaving behind a methylene radical which may participate in crosslinking. A possible reaction sequence is shown in equations 15-17.

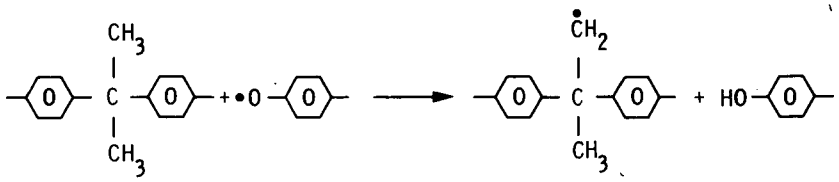

(15)

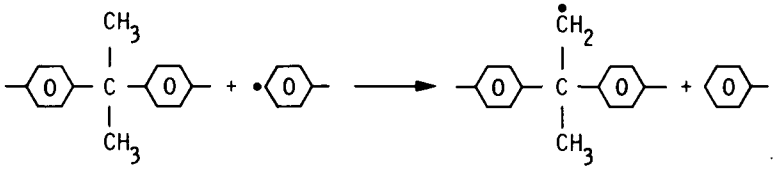

(16)

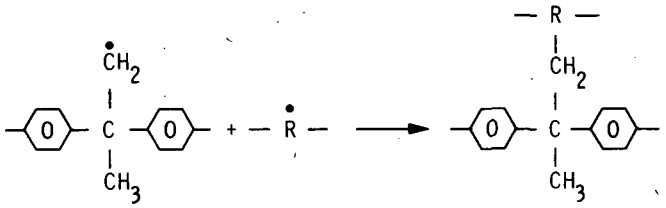

(17)

The isopropylidene linkage may also represent a point of main chain scission as shown in equation 18, although no direct evidence of this reaction has been observed in this study.

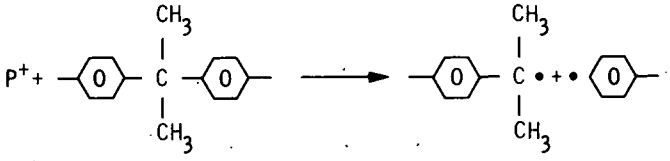

(18)

Phenyl radicals created as in equations 12, 13, and 18 may simply abstract hydrogen atoms forming monosubstituted aromatics or two of them may recombine forming a strained biphenyl linkage, as shown in equation 19.

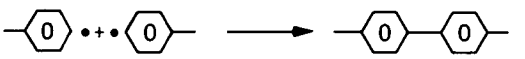

(19)

A number of other possible radicals and radical reactions have been postulated in the literature.[42-45] Indeed it is expected that some or all of these as well as other previously unknown reactions occur as a result of proton irradiation. However, no direct evidence has been observed for these in this work.

B. Poly(1-vinylnaphthalene)

P1VN is a glassy aromatic polymer whose structure is shown below.

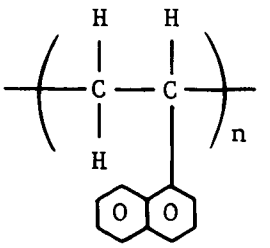

This material has been utilized previously as a model compound for more complex aromatic polymers in UV[50] and electron beam[33] radiolysis studies. Since it is a very brittle material, mechanical tests are difficult and consequently were not included as part of this study. Instead, the emphasis was on sol-gel, HPLC and spectroscopic analysis of irradiated samples.

1. Sol-gel and HPLC Studies

An insufficient number of samples were available to do a complete sol-gel study including a Charlesby-Pinner plot; however, a few samples with exposure of up to several thousand Mrad of proton radiation were investigated and the results are shown in Table VI. Clearly, in PlVN, the gel fraction increases much more slowly with dose than in the case of polysulfone (see Table IV).

HPLC analysis of the soluble fraction of exposed samples was carried out in two parts. First, high molecular weight exclusion columns were used to look at changes in the molecular weight of the remaining soluble polymer and then low molecular weight columns were used to look at the small fragments produced.

The chromatograms of the soluble fraction of a control and two irradiated samples using the high molecular weight columns are shown in Figure 13. It is apparent that in the sample receiving a dose of 738 Mrad, there has been both chain scission and crosslinking. Furthermore, the increase in Mw and decrease in Mn are indicative of non-randomness in the radiation induced degradation. The chromatogram of the highly irradiated (5517 Mrad) sample shows a very broad distribution of molecular weights ranging from greater than 100,000 to less than 300. Clearly, the soluble fraction in this case contains mostly low molecular weight material. The high molecular weight material has presumably been locked up in a gel.

Similarly, Figure 14 shows the chromatograms of the soluble fraction of three PlVN samples recorded using the low molecular weight columns. In the control sample only high molecular weight material is detected. In the irradiated samples, there is a considerable amount of low molecular weight material present including three discrete features with retention times of approximately 17.5, 19, and 20.5 minutes. Calibration using known standards

Table VI. Sol-Gel Study on Proton Irradiated P1VN Samples

Dose	Soluble Fraction
0	1.0
203	1.0
660	0.82
1092	0.67

shows that these features correspond to molecular weights of 182, 155, and 127 gm/mole respectively with an uncertainty of ±2 gm/mole. Based on the known structure of the polymer and the observed molecular weights it is believed that the fragments correspond to naphthalene (MW = 128), ethylnaphthalene or vinylnaphthalene (MW = 156 or 154) and naphthylbutane, naphthylbutene, or naphthylbutadiene (MW = 184, 182, or 180).

2. Spectroscopic Characterization

Spectroscopic analysis of irradiated P1VN samples yielded relatively fewer interesting results than in the case of polysulfone. This probably reflects the fact that in a pure hydrocarbon, like P1VN, it is harder to distinguish the spectra of degradation products from the control material than in something like polysulfone where significant changes in elemental composition may be expected.

On line UV-visible absorption spectra run on the individual HPLC components of the sample exposed to 6610 Mrads using the low molecular weight columns show that the spectrum of the lowest molecular weight fragment (Figure 15) is in good agreement with that of naphthalene. Due to their low concentration, good spectra of the 17.5 and 19 minute components could not be obtained. However, they both show broad red shifted (10-20 nm) absorption

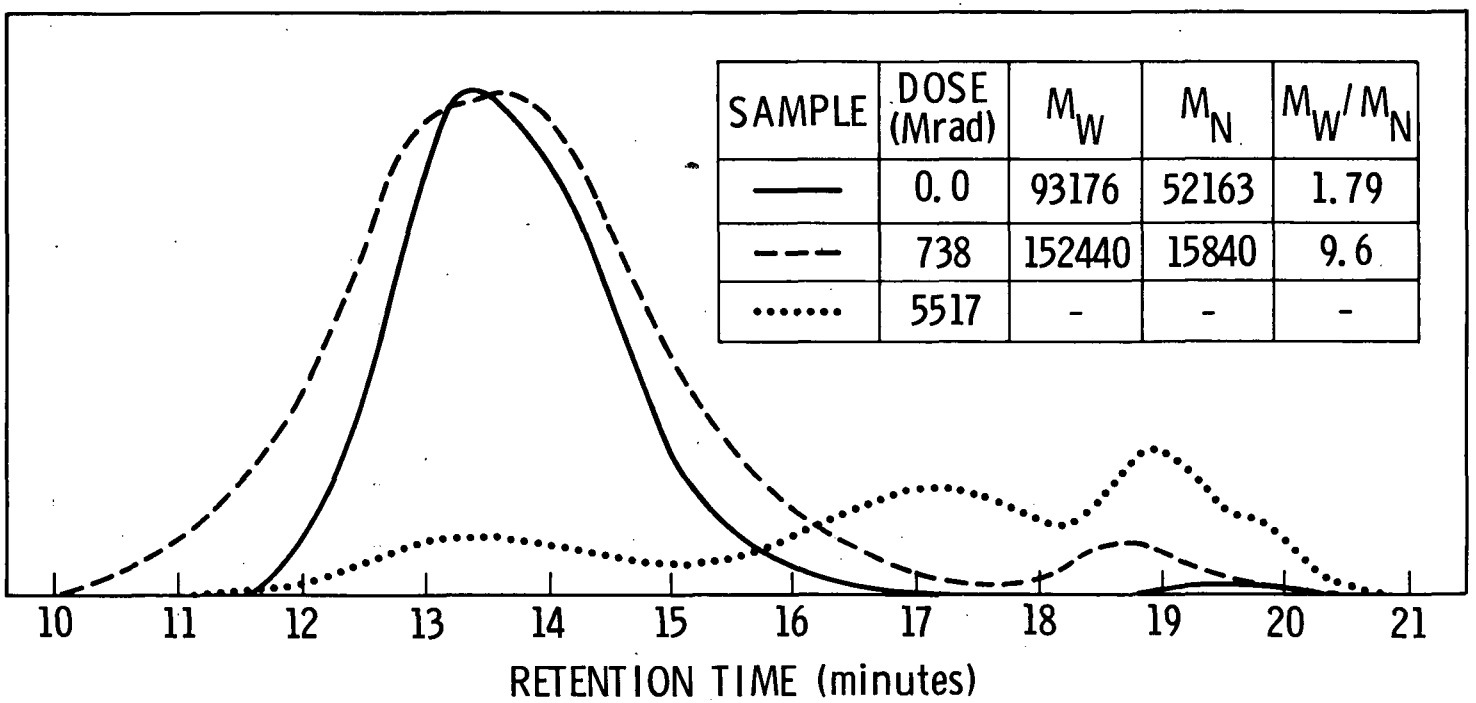

Figure 13. Chromatograms of the Soluble Fraction of Control and Proton Irradiated PlVN Using High Molecular Weight Columns

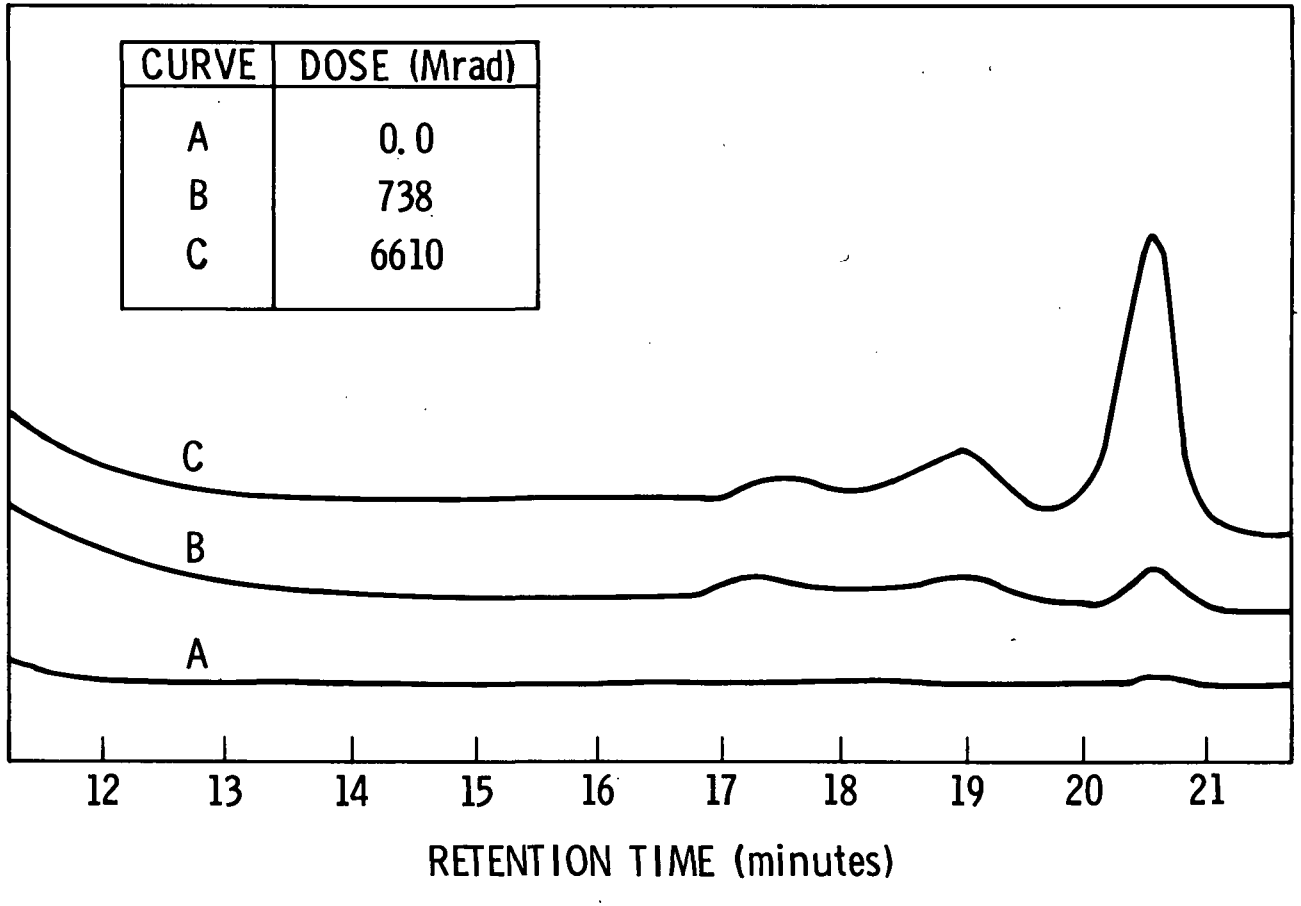

Figure 14. Chromatograms of the Soluble Fraction of Control and Proton Irradiated P1VN Using Low Molecular Weight Columns

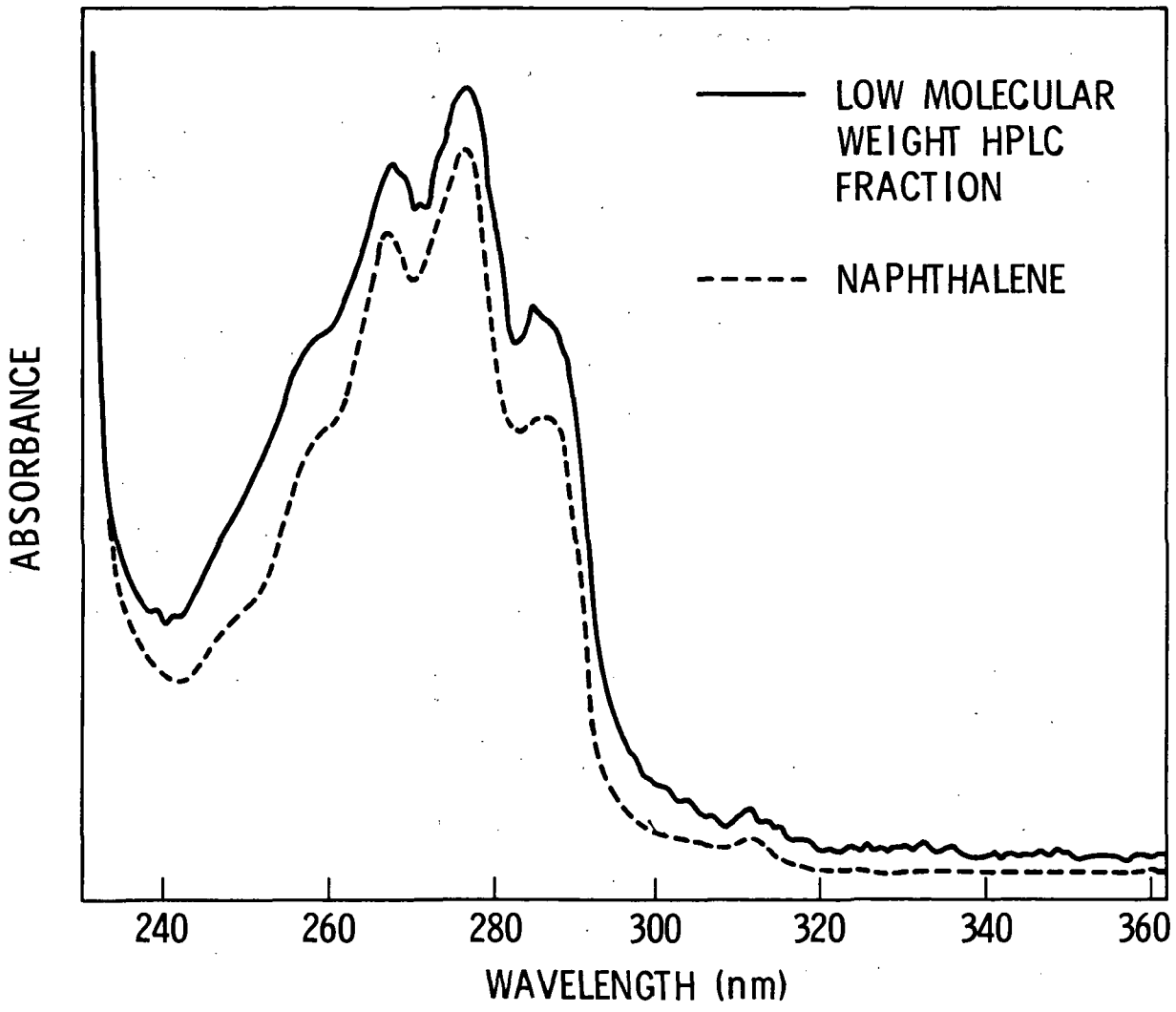

Figure 15. UV-Visible Absorption Spectra of Naphthalene and Lowest Molecular Weight Fragment Separated from Proton Irradiated P1VN by HPLC

features in the same general wavelength region as naphthalene with no structure visible in the noise. Clearly, they are naphthalene containing species and the broadening and red shifting are consistent with unsaturation in the side chains. Given the quality of the data, however, it is not possible to unambiguously determine the nature of these compounds.

FTIR spectra were run on the soluble fractions of control and irradiated samples following extraction with methylene chloride. The spectra, even at the highest doses, were virtually identical. The only clearly distinguishable change is the appearance of a relatively weak -OH absorption band near 3500 cm^{-1} in irradiated samples. This probably results from the interaction of atmospheric oxygen with the material after it was removed from the evacuated irradiation chamber. Typical FTIR spectra from a control and an exposed (5517 Mrad) sample in the -OH region are shown in Figure 16.

UV-visible absorption spectra run on exposed samples showed very little change relative to the controls. Only one sample, exposed to more than 10,000 Mrads, showed any noticeable yellowing. In-situ emission spectra from P1VN films recorded during irradiation showed results similar to those obtained in electron beam[33] studies. Figure 17a shows a typical spectra recorded at a dose of 500 Mrads. The emission, which peaks at ~400 nm, is clearly from the P1VN excimers. Exposure of films doped with anthracene results in spectra like that shown in Figure 17b. The P1VN emission is largely gone and is replaced with anthracene emission. This is indicative of long range excitation transport in this material which may be utilized to achieve stabilization via energy trapping and dissipation by dopant species.

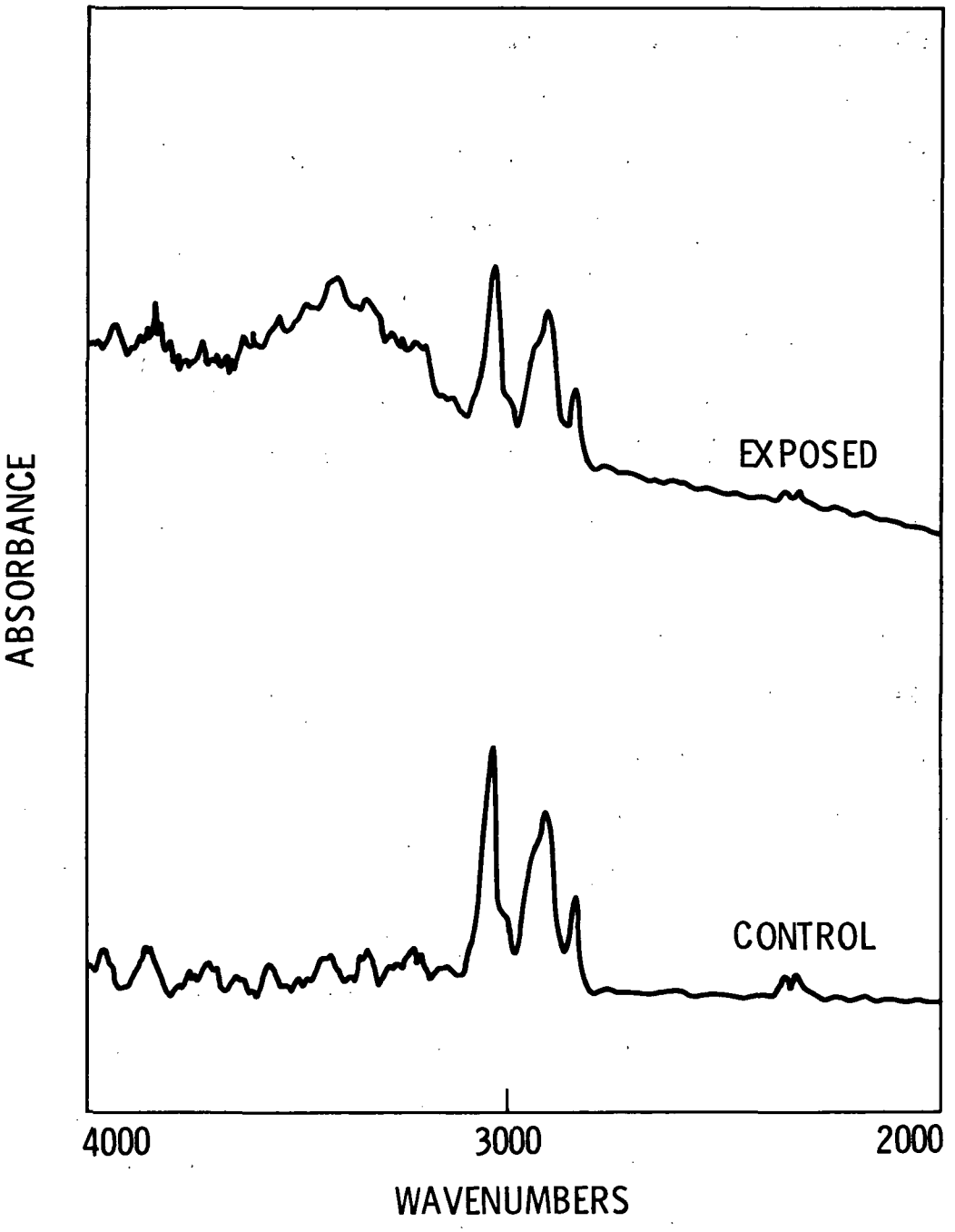

Figure 16. Typical FTIR Spectra of Control and Proton Irradiated P1VN in OH Stretching Region

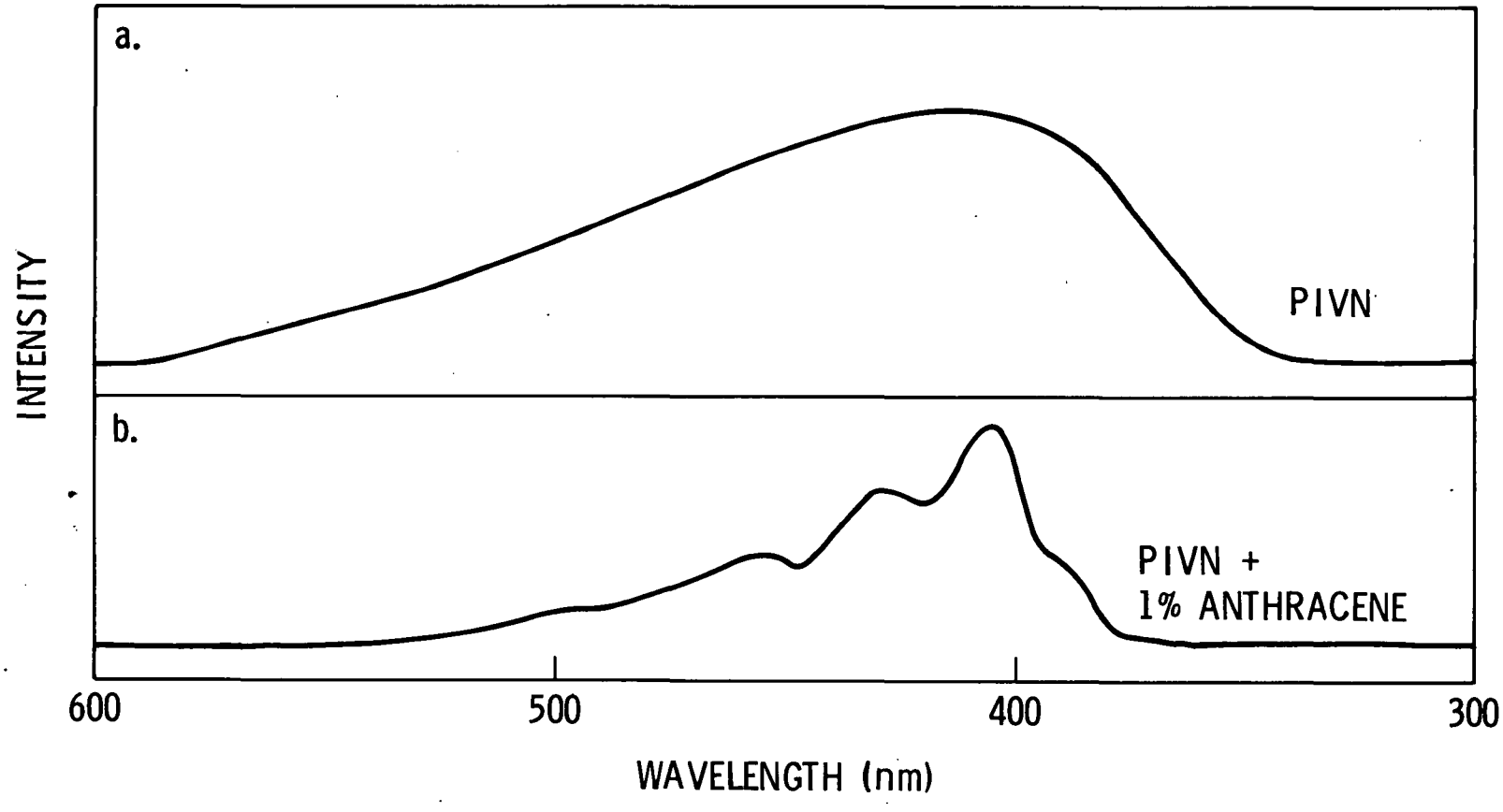

Figure 17. In-situ Emission Spectra of PlVN and Anthracene Doped PlVN Recorded During Proton Bombardment

Finally, proton irradiated P1VN samples exhibit a persistent ESR signal as shown in Figure 18. This radical species has a g-value of 2.0050 and is similar to that observed in irradiated polystyrene. It is assigned to the quite stable tertiary carbon radical shown below.

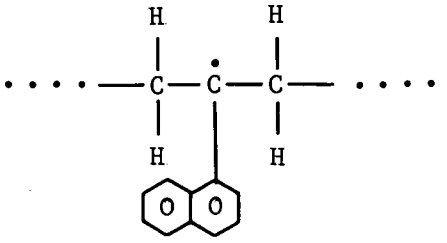

This radical signal decays away over a period of days in air and weeks in vacuum.

3. Discussion

Poly(1-vinylnaphthalene) has been found to be relatively stable under energetic proton bombardment. This is typical of highly aromatic materials. Both chain scission and crosslinking have been found to have occurred in irradiated samples. These processes appear to have involved only the backbone of the napthalene moieties intact.

The major low molecular weight fragment observed in irradiated P1VN is naphthalene, which is presumably formed by a reaction such as is shown in equation 20.

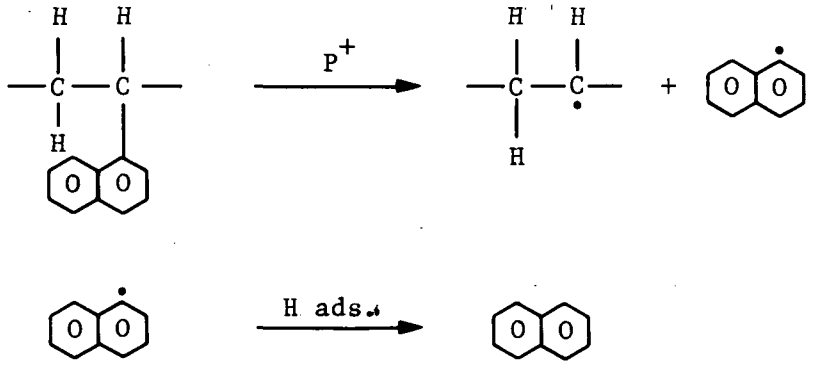

(20)

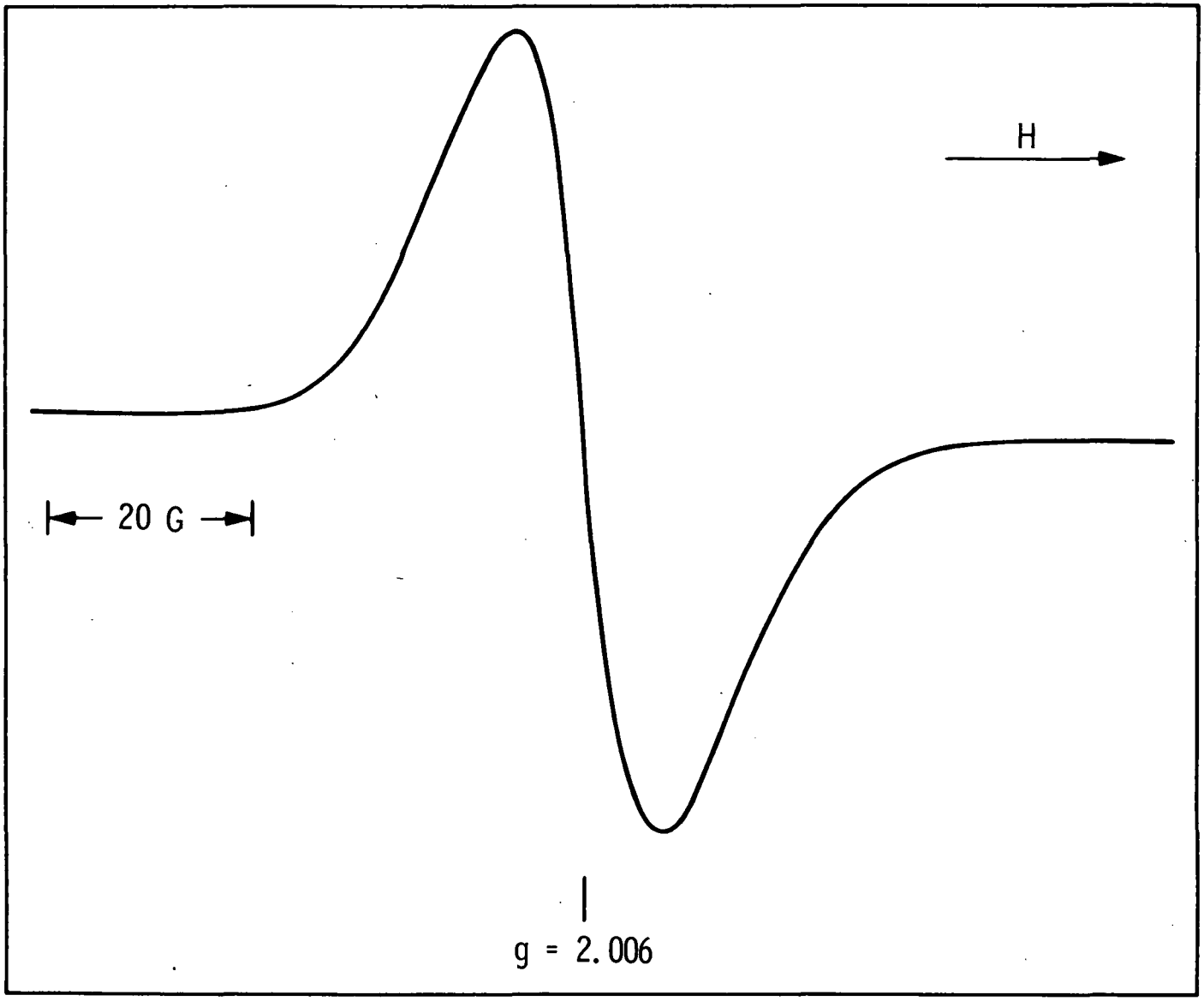

Figure 18. ESR Spectrum of Proton Irradiated P1VN

Crosslinking could then occur from the alkyl radical left where the naphthalene split off or from a tertiary radical created as shown in equation 21 and observed in the ESR spectrum.

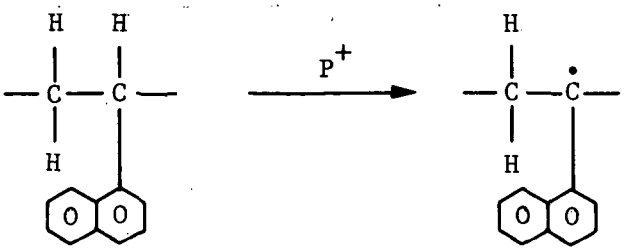

(21)

The presence of higher molecular weight fragments (alkylnaphthalenes) is indicative that larger pieces of the backbone can be split off. It is not clear whether such processes are concerted (occur in a single step) or whether they occur as a result of a secondary reaction (i.e., hydrogen abstraction) leaving behind an unstable species which then dissociates.

C. Other Polymers

1. Polymethylmethacrylate (PMMA)

PMMA showed by far the most change of any of the polymers in this study. Doses of a few hundred Mrads reduced initially sturdy transparent films to a brittle, flakey, opaque material. At high doses (> 1000 Mrads), frequently only powder was found in the bottom of the irradiation chamber.

Initial concern that PMMA might be particularly sensitive to temperature increases prompted a study as a function of dose rate. Figure 19 is a photograph of a sample that shows severe damage after exposure to a beam current of only 8.4 nA/cm^2 (far below the calculated "safe" beam current of 75 nA/cm^2). The total accumulated dose on this sample was 333 Mrads. Microscopic examination of this sample revealed that the "graininess" observed is really bubbles present in the material resulting from the formation of volatiles during irradiation.

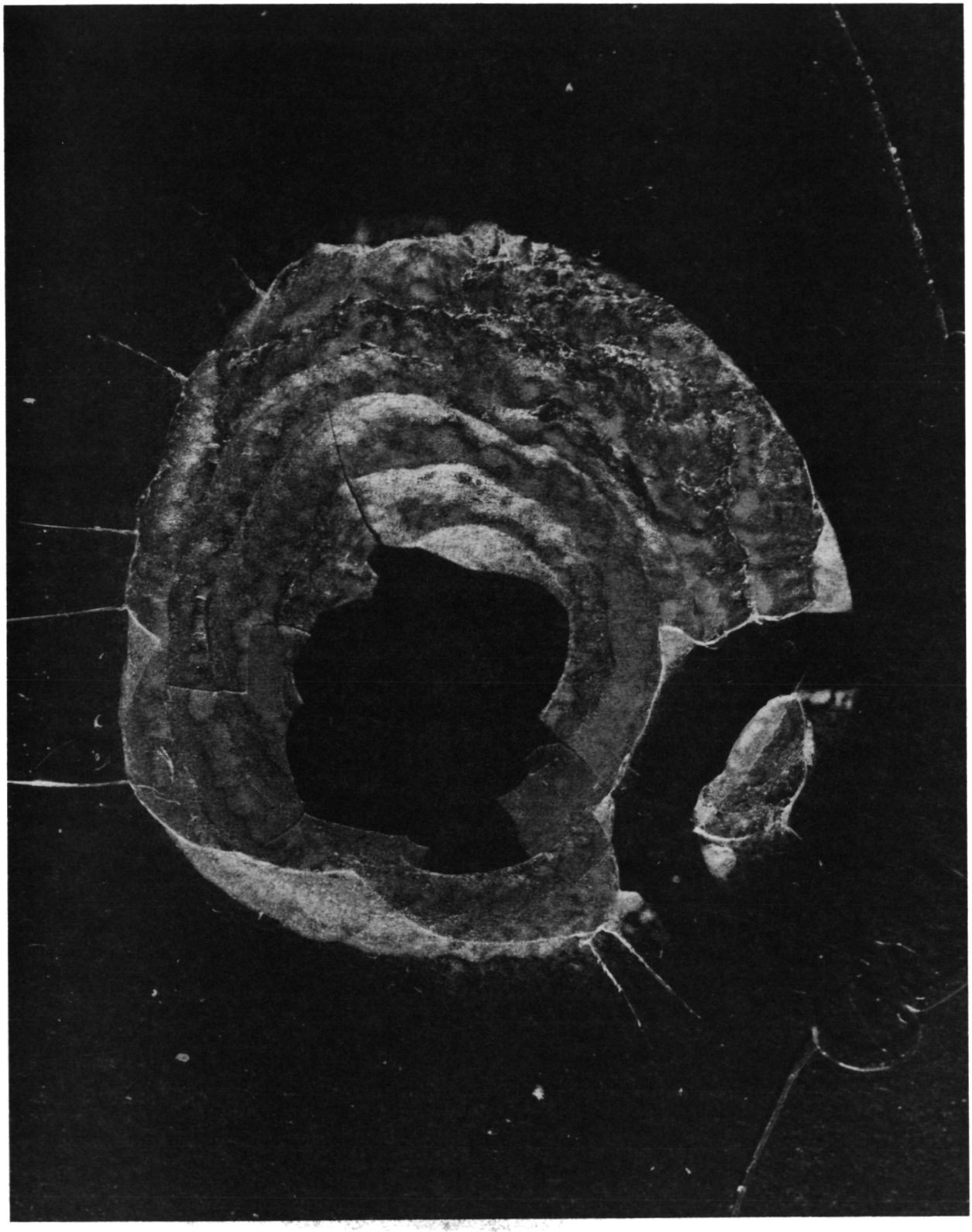

Figure 19. Photograph of PMMA Film Exposed to 333 Mrads of Proton Radiation

HPLC analysis of irradiated PMMA showed no evidence of crosslinking. Only chain scission was observed. Initial molecular weights were in the range of 500,000 - 800,000 while samples receiving 7500 Mrads of proton radiation showed no material of >20,000 molecular weight remaining. PMMA probably unzips; however, there is no direct evidence of a monomer which would have been pumped away if it were formed in the evacuated irradiation chamber.

Diffuse reflectance FTIR carried out on control and exposed samples showed some differences. In Figure 20 it can be seen that features at 2998 cm^{-1}, 1483 cm^{-1} and 1060 cm^{-1} present in the control are reduced in the irradiated material. Koenig[51] has assigned the two higher frequency bands to $C-CH_3$ vibrations and the 1060 cm^{-1} band to a C-C skeletal motion. It is apparent that loss of $-CH_3$ on the polymer backbone is an important process in the proton degradation of PMMA.

The UV-visible absorption spectrum of irradiated PMMA dissolved in methylene chloride is shown in Figure 21. Considerable yellowing is apparent. This may be due to increased unsaturation and conjugation resulting from proton damage. Such an explanation is supported by postirradiation emission spectroscopy. The fluorescence spectra of a control and irradiated PMMA sample are shown in Figure 22. The irradiated sample shows a considerably broadened red shifted emission indicative of extended conjugation of the carbonyl.

PMMA was the only nonaromatic material investigated. The extreme level of damage to it lends strong support to the notion that aromatic groups tend to make materials more radiation stable.

2. Epoxy

Narmco 5208 epoxy consists primarily of a tetrafunctional epoxide (tetraglycidyl-diamino-diphenyl-methane) cured with diamino-diphenyl-sulfone. This is a very durable material. Since it is a thermoset resin, it has no soluble fraction initially and none developed as a result of

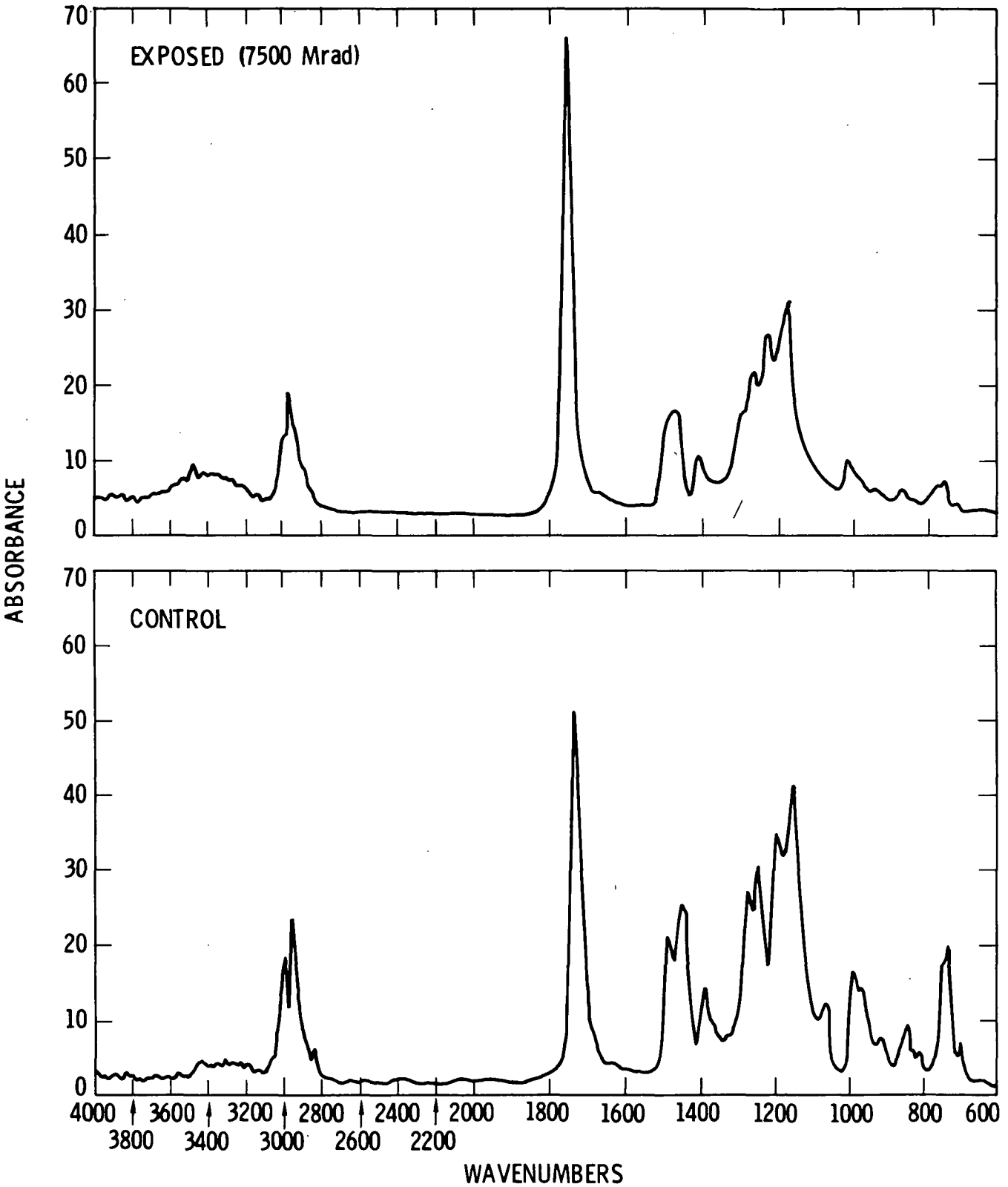

Figure 20. FTIR Spectra of Control and Proton Irradiated PMMA Films

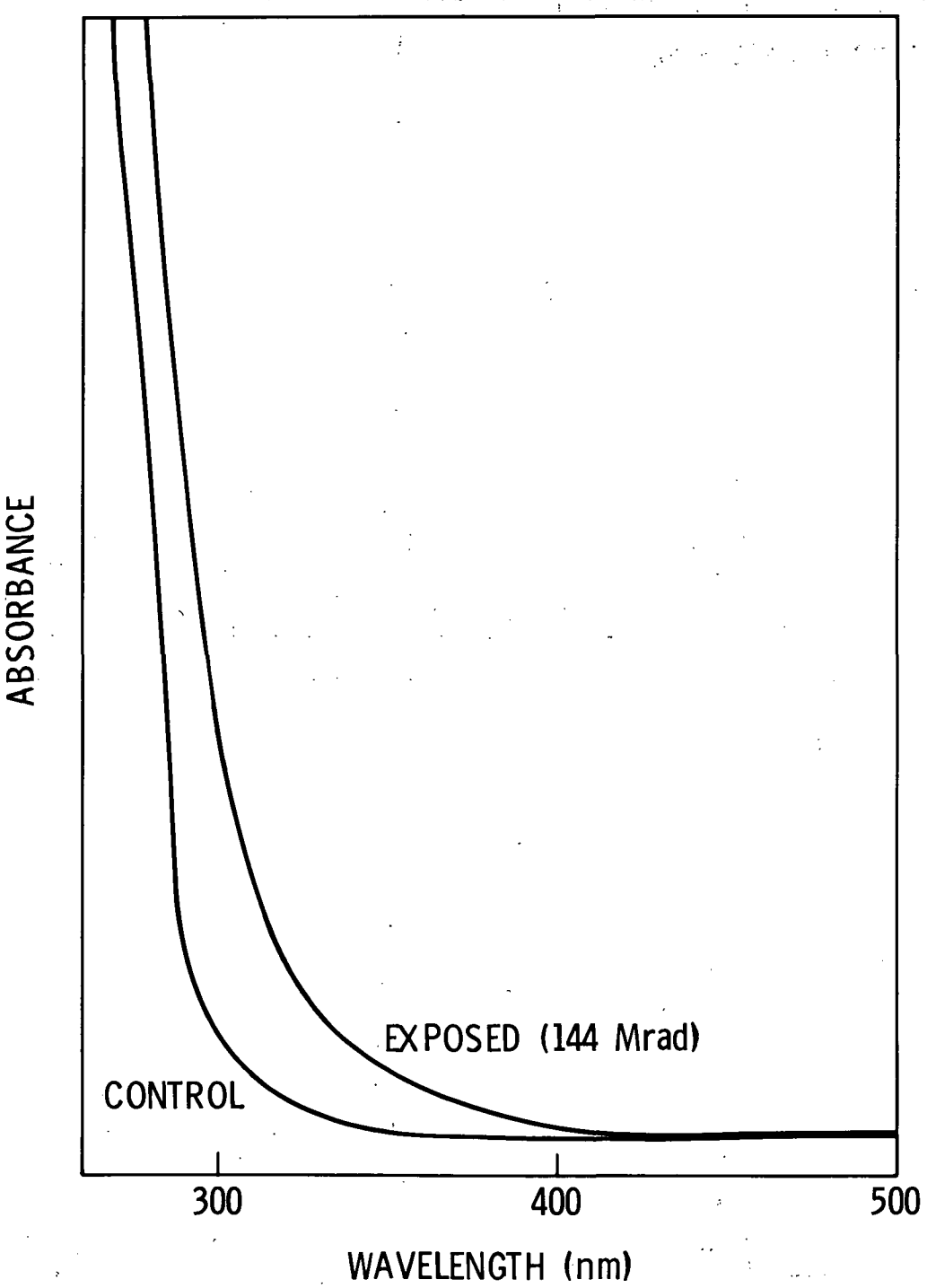

Figure 21. UV-Visible Absorption Spectra of Control and Proton Irradiated PMMA

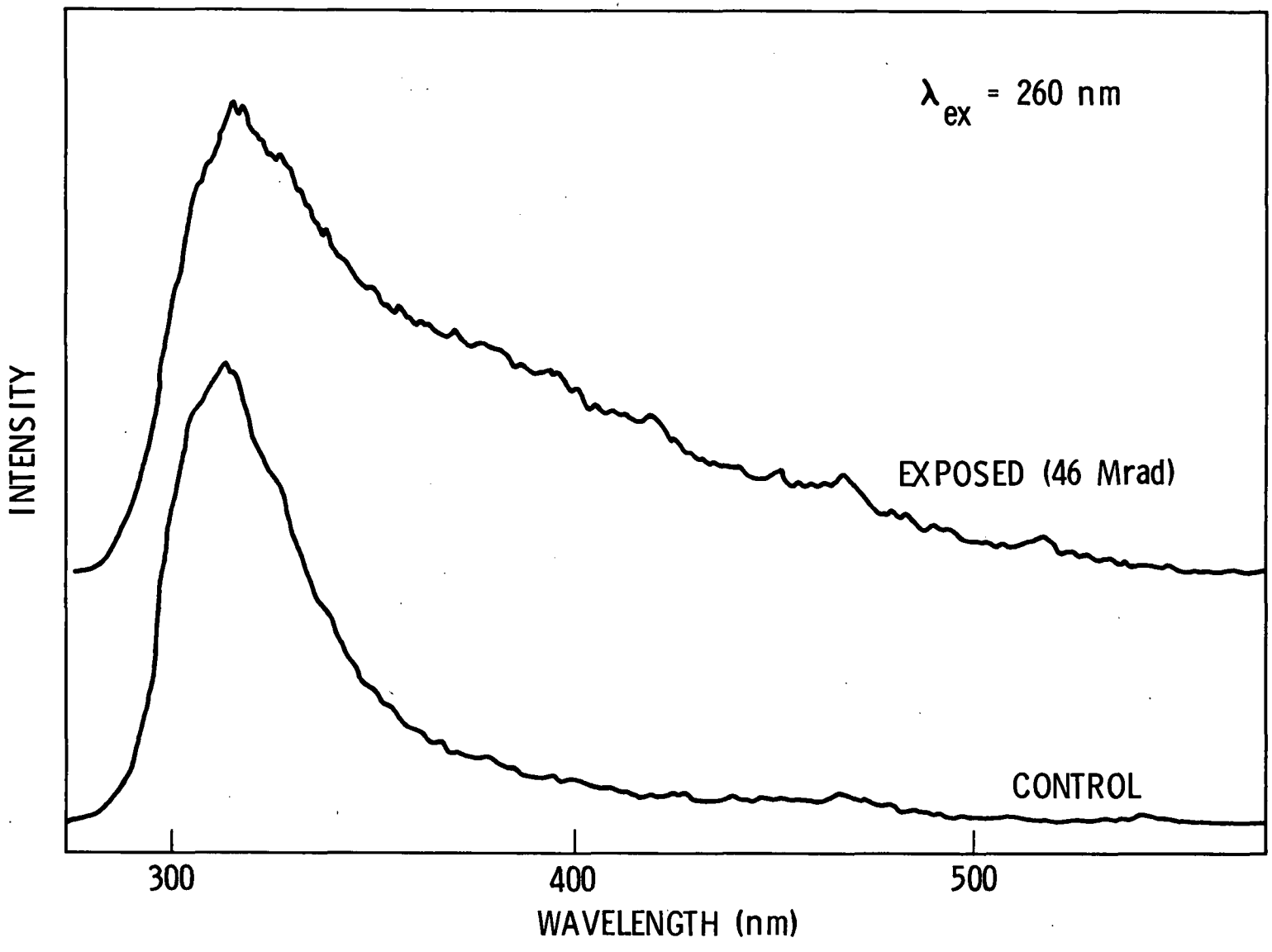

Figure 22. Fluorescence Spectra of Control and Proton Irradiated PMMA Films Recorded Following Bombardment

irradiation. Furthermore, there was no measurable change in mechanical properties or FTIR spectra up to doses of several thousand Mrads.

Only two tests showed any clearly identifiable changes in this material resulting from proton bombardment. The UV-visible absorption spectrum of the irradiated material showed a shift in the absorption edge to longer wavelength which is indicative of further radiation induced cure of the system. Also, an absorption band appeared at ~635 nm (see Figure 23) which decayed away as a function of time. A plot of $1/\varepsilon c$ ($\varepsilon \equiv$ molar extinction coefficient, $c \equiv$ concentration in moles/liter) vs. time is given in Figure 24 and is seen to be linear which is evidence for a second order decay process.

The ESR spectrum of irradiated epoxy shows a radical species which also decays away over a matter of weeks (see Figure 25). The actual decay rate was not measured in these experiments. The same radical species has been reported[52] following e-beam bombardment of this material. Time dependent studies of the decay show a slow component with a second order decay constant of $1.2 \pm 0.4 \times 10^{-4}$ liters/mole-s. It is believed that the same species is responsible for the ESR signal and the absorption band at 635 nm. If the absorbing radical has a typical extinction coefficient of 10^4 liters/mole-cm then from the slope of the line in Figure 24 a decay constant of 1.2×10^{-4} liters/mole-s is obtained. The decay of this species is probably a recombination of two radicals to form a new crosslink, thus giving a second order decay and further extending the amount of radiation induced cure.

3. Kapton

A few Kapton samples were exposed with dose levels reaching as high as 9000 Mrads. None of the diagnostic tests revealed any changes. This is not too surprising in light of the fact that this material is a proven radiation stable polymer with a threshold for damage in excess of 10^{10} rads.[53]

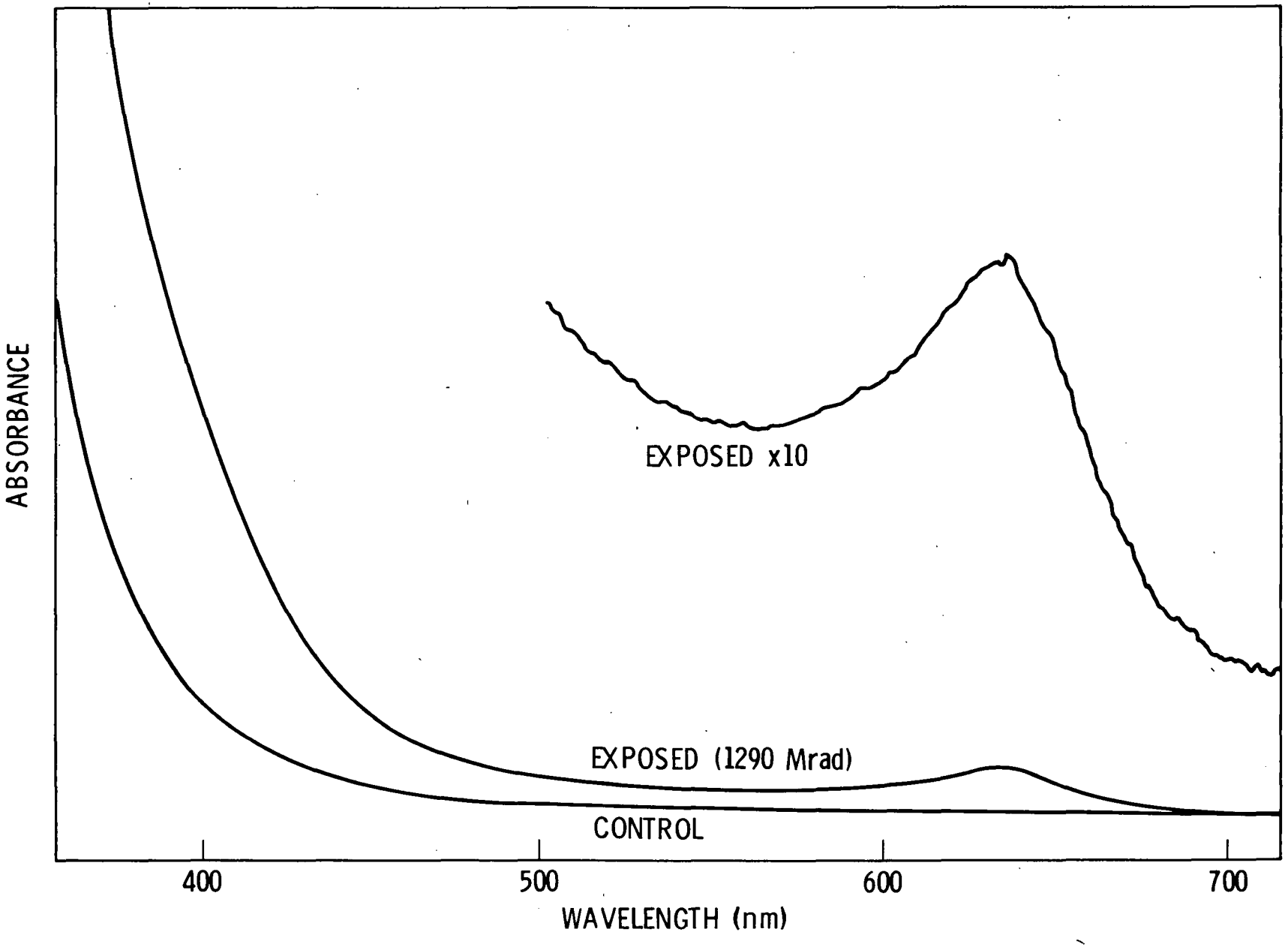

Figure 23. UV-Visible Absorption Spectra of a Control and a Proton Irradiated Epoxy Sample

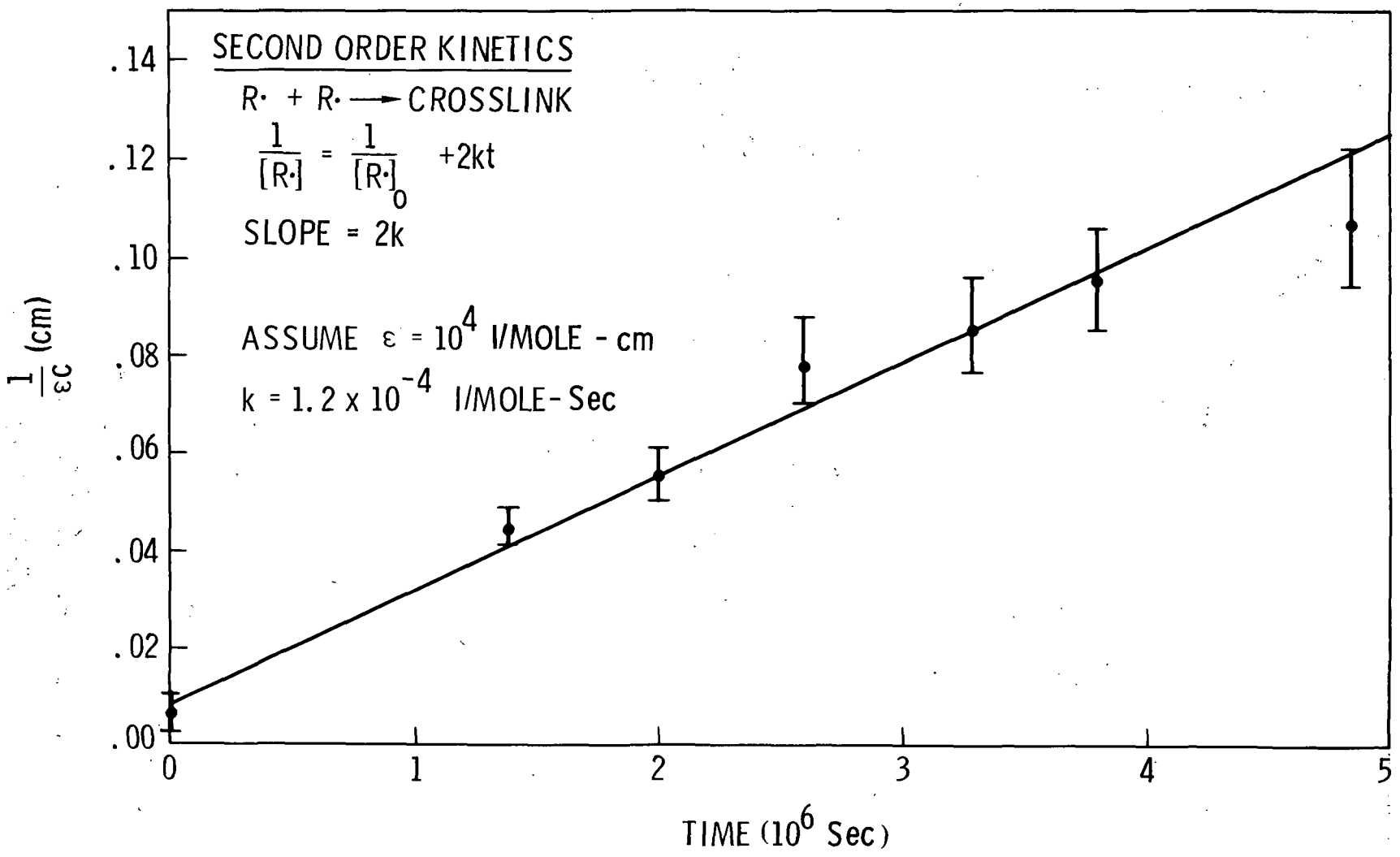

Figure 24. Plot of 1/εc vs Time for the 635 nm Absorption Band Observed in Proton Irradiated Epoxy

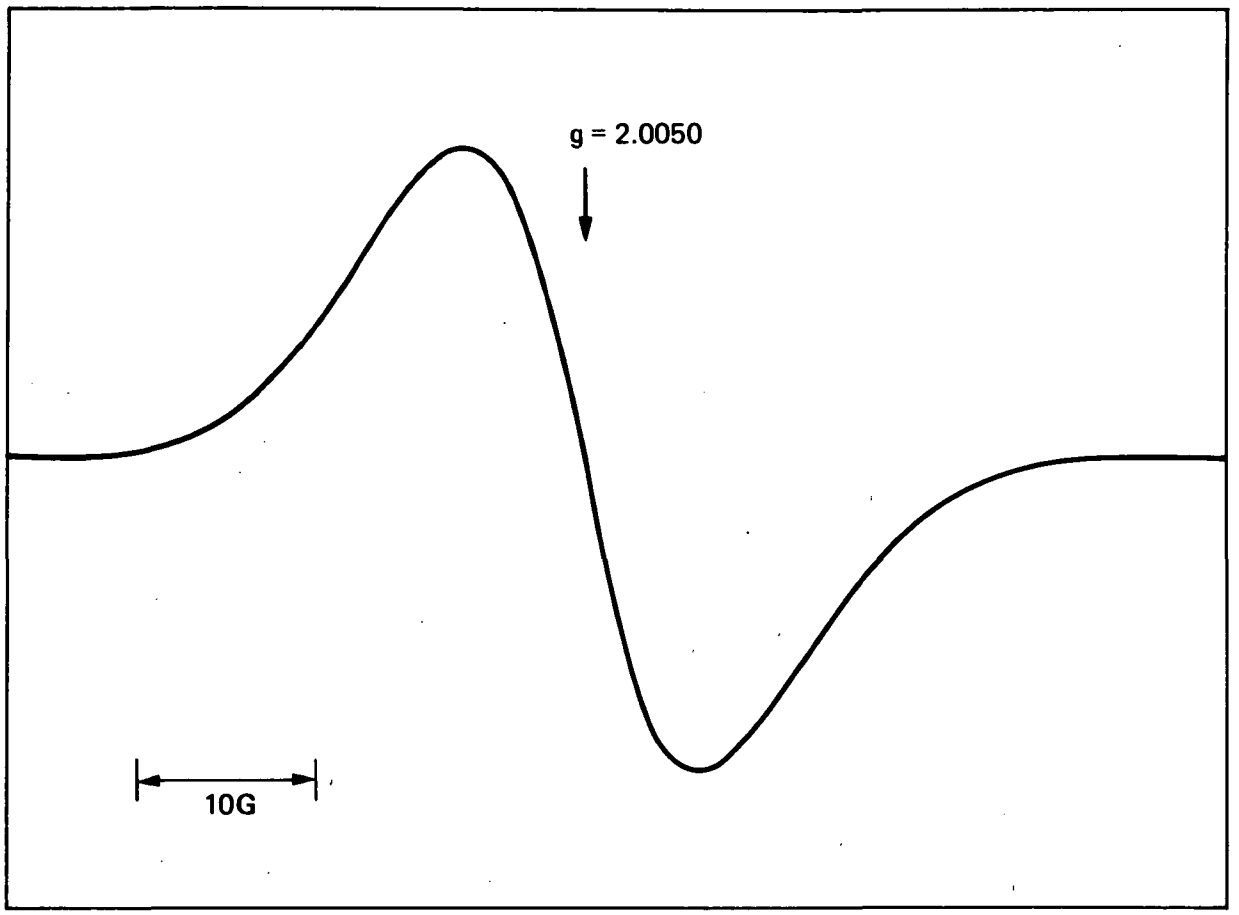

Figure 25. ESR Spectrum of Proton Irradiated Epoxy Recorded 48 Hours After Bombardment

VI CONCLUSIONS

The results of this study clearly indicate that many organic polymers exhibit a sensitivity to energetic proton bombardment. Doses in the range of tens to thousands of Mrads have been observed to cause changes in the mechanical, physical, chemical, and optical properties of various materials tested. The nature, magnitude, and effects of such changes must be understood if organic polymers are going to be utilized for long term missions in space.

The effects of proton irradiation on polymers are in many ways similar to those observed for other forms of ionizing radiation. That is, proton bombardment generally results in crosslinking, chain scission or both in the material. A considerable amount of complex chemistry, including ion formation, radical formation, hydrogen abstraction, bond scission leading to loss of low molecular weight volatiles, etc., generally precedes these processes. With a detailed understanding of the nature of these processes leading to degradation, certain general statements could be made concerning the potential radiation stability of a given material. For example, polymers with many aromatic groups generally show more radiation durability than those without such moieties. This, however, is not true in all cases. Lexan, an aromatic polycarbonate, for example, is well known to be very unstable to radiation and is actually used in dosimetry. Clearly, much more work is necessary.

The damage incurred as a result of exposure to ionizing radiation is a function of penetration depth. Considering UV, protons, and electrons to be the major components of space radiation, it is found that in polymeric materials, their ranges generally are in the order UV < protons < electrons. Of course, the energies of the radiations are of considerable importance in determining the actual range. For a given incident dose, protons are found to do more damage to thin films than electrons of the same energy. This is

simply related to the fact that in polymers, the range of a 3 MeV proton, for example, is ~ .01 cm while the range of a 3 MeV electron is 1.3 cm and thus the density of deposited energy is two orders of magnitude higher for protons. The practical significance of this is that heavier, lower energy particles are more damaging to coatings, blankets, and outer surfaces while lighter more energetic particles may penetrate and degrade bulk materials.

In relation to designing future tests, three critical issues are apparent: vacuum, temperature, and acceleration factor. Clearly, to simulate a true space environment, oxygen must be excluded from the irradiation chamber. Oxygen may serve to react with some energetic species or it may serve to quench radicals, excited states, etc., thus greatly altering the nature and rate of various degradation processes. Also, temperature must be controlled, particularly at high dose rates, in order to minimize thermally induced reacions. Simple cooling techniques are available to solve this problem. Finally, the most poorly understood issue is the choice of how much the dose rate can be accelerated and still provide a reasonable representation of the space environment. Our conclusion is, that since for these lighter particles energy is deposited in little pockets ("spurs") as the particle passes through the matrix, a reasonable acceleration factor is one which precludes two spurs forming and interacting with each other during a time in which excited species are still present. If one knows the lifetime of the species in the spur and the dose rate, then a probability of creating another spur within a given radius and time can be estimated. For short lived species (10^{-12} - 10^{-6} s) this is not of much concern; however, for very long lived radicals and ions this problem may be very limiting.

VII ACKNOWLEDGEMENTS

The authors would like to thank Professor Charles Barnes and Mr. R. Ebert of the California Institute of Technology for many useful discussions prior to and during these tests and for operation of the proton beam accelerator. Also, we would like to thank Ms. K. Oda and Mr. M. Cizmecioglu for overseeing the mechanical testing and Dr. F. D. Tsay for running the ESR spectrometer.

VIII REFERENCES

1. A. Charlesby, Proc. Roy. Soc. (London), A215, 187 (1952).
2. A. Charlesby, Nature, 171, 167 (1953).
3. A. Charlesby and M. Ross, Proc. Roy. Soc. (London), A217, 122 (1953).
4. A. Charlesby and N. H. Hancock, Proc. Roy. Soc. (London), A218, 245 (1953).
5. L. A. Wall and M. Magat, J. Chem. Phys., 50, 308 (1953).
6. A. Charlesby and M. Ross, Nature, 171, 1153 (1953).
7. E. N. Teleshov, Thesis, Physiochemical Scientific Research Institute, Moscow (1963).
8. F. Williams, in "Fundamental Processes in Radiation Chemistry," ed, P. Ausloos, Interscience, New York (1968).
9. R. M. Keyser, K. Tsuji, and F. Williams, Macromolecules, 1, 3289 (1968).
10. R. M. Keyser and F. Williams, J. Phys. Chem., 73, 1623 (1969).
11. G. Geuskens, D. Fuld, and C. David, Makromolekulare Chemie, 160, 135 (1972).
12. R. H. Partridge, J. Chem. Phys., 52, 1277 (1970).
13. M. Dole, G. G. A. Bohm, and D. C. Waterman, Europ. Polym. J. Suppl., (1969), p. 93.
14. D. C. Waterman and M. Dole, J. Phys. Chem., 74, 1913 (1970).
15. D. C. Waterman and M. Dole, J. Phys. Chem., 74, 1906 (1970).
16. M. Dole and G. G. A. Bohm, Advan. Chem., Ser., 82, 525 (1968).
17. R. E. Michel, F. W. Chapman, and T. J. Mao, J. Polymer Sc., Part A-1, 5, 677 (1967).
18. J. Wieske and H. Heusinger, J. Polymer Sci., Part A-1, 7, 995 (1969).

19. R. Salovey, J. P. Luongo, and W. A. Yager, Macromolecules, 2, 198 (1969).

20. D. H. Phillips and J. C. Schug, J. Chem. Phys., 50, 3297 (1969).

21. R. K. Swank and W. L. Buck, Phys. Rev., 91, 927 (1953).

22. F. H. Brown, M. Furst, and H. Kallman, U.S. Atomic Energy Commission, TID-7612, 37 (1961).

23. Robert F. Cozzens and Robert B. Fox, J. Chem. Phys., 50, 1532 (1969).

24. Robert B. Fox, Thomas R. Price, and Robert F. Cozzens, J. Chem. Phys., 54, 79 (1971).

25. J. S. Aspler, C. E. Hoyle, and J. E. Guillet, J. Am. Chem. Soc., 11, 925 (1978).

26. A. Gupta, R. Liang, J. Moacanin, D. Kliger, R. Goldbeck, J. Horwitz, and V. Miskowski, European Polymer J., 17, 485 (1981).

27. A. N. Goryacher and L. N. Pankratova, Khimiya Vysokikh Energii, 4, 542 (1970).

28. A. Charlesby, A. R. Gould, and K. J. Ledbury, Proc. Roy. Soc. (London), A277, 348 (1964).

29. A. B. Zverev, Khimiya Vysokikh Energii, 5, 453 (1969).

30. D. R. Coulter, M. V. Smith, F. D. Tsay, A. Gupta, and R. E. Fornes, J. App. Poly. Sci., 30, 1753 (1983).

31. F. A. Makhlis, in "Radiation Physics and Chemistry of Polymers," J. Wiley and Sons, New York (1975).

32. L. E. Seiberling, J. E. Griffith, and T. A. Tombrello, Rad. Effects, 52, 201 (1980).

33. D. R. Coulter, R. H. Liang, S. DiStefano, J. Moacanin, and A. Gupta, Chem. Phy. Lett., 87(6), 594 (1982).

34. H. H. Andersen and J. F. Ziegler, in Hydrogen: Stopping Powers and Ranges in all Elements, Pergamon Press, New York, (1977).

35. J. E. Ferl and E. F. Long, Jr., IEEE Trans. Nucl. Sci., NS-28, 4119, (1981).

36. S. A. T. Long and E. R. Long, Jr., private communication.

37. J. B. Marion and B. A. Zimmerman, Nuc. Instr. and Math., 51, 93 (1967).

38. A. Charlesby and S. H. Pinner, Proc. Roy. Soc. (London), Ser. A., 249, 367 (1959).

39. A. Charlesby, "Atomic Radiation and Polymers," Pergamon Press, London (1960).

40. J. R. Fried and H. Kalkanoglu, J. Poly. Sci., Poly. Lett. Ed., 20, 381 (1982).

41. P. R. Young, B. A. Stein, and A. C. Chang, Proc. 28th Natl. SAMPE Symposium, 824 (1983).

42. P. B. Ayscough, K. J. Ivin, and J. H. O'Donnell, Trans. Faraday Soc., 61, 1110 (1965).

43. A. R. Lyons, M. C. R. Symons, and J. K. Yandell, Makromolek. Chem., 157, 103 (1972).

44. J. R. Brown and J. H. O'Donnell, J. App. Polym. Sci., 19, 405 (1975).

45. J. R. Brown and J. H. O'Donnell, J. App. Polym. Sci., 23, 2763 (1979).

46. B. Santos and G. F. Sykes, Proc. 13th National SAMPE Tech. Conf., 256 (1981).

47. T. Sasuga, N. Hayakawa, and K. Yoshida, J. Polym. Sci., Polym. Phys. Ed., 22, 529 (1984).

48. W. Gordy, "Theory and Applications of Electron Spin Resonance," Wiley and Sons, New York (1980).

49. D. R. Coulter, unpublished result.

50. A. Gupta, R. Liang, J. Moacanin, D. Kliger, R. Goldbeck, J. Horwitz, and V. Miskowski, Eur. Poly. J., 17, 485 (1981).

51. S. Dirlikov and J. Koenig, App. Spect., 33(6), 551 (1979); S. Dirlikov and J. Koenig, App. Spect., 33(6), 555 (1979).

52. K. R. Schaffer, R. E. Fornes, R. D. Gilbert, and J. D. Memory, Polymer, 25(1), 54 (1984).

53. W. M. Rowe, in "Sail Film Materials and Support Structures for a Solar Sail - a Preliminary Design - Volumn IV," JPL Solar Sail Development Program Report JPL (internal document) #720-9 (1978).